

Supporting Information

Carbazole-based artificial light-harvesting system for the photocatalytic cross-coupling dehydrogenation reaction

Guangping Sun,* Menghang Li, Lijuan Cai, Jinli Zhu, Yanfeng Tang* and Yong Yao*

School of Chemistry and Chemical Engineering, Nantong University, Nantong 226019, China.

E-mail: sunguangping1989@ntu.edu.cn; tangyf@ntu.edu.cn; yaoyong1986@ntu.edu.cn.

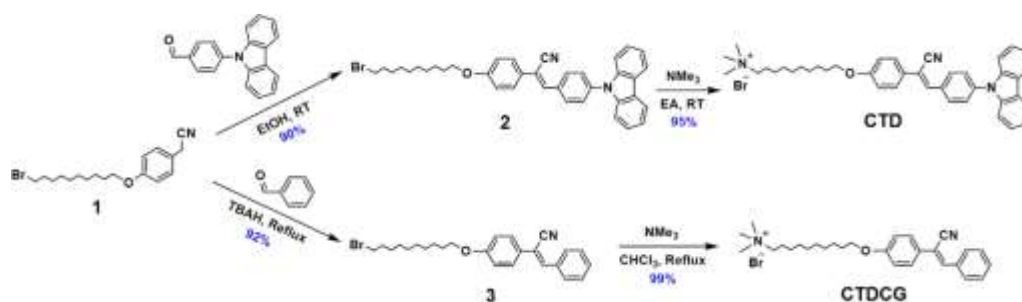
Table of Contents

1. General information	S2
2. Synthesis of CTD and CTDCG	S2
3. Host-guest interaction of WPP5 and CTD	S11
4. Fabrication of nanoparticle.....	S11
5. Zeta potential results of WPP5-CTD and WPP5-CTD-ESY	S11
6. Absorbance spectrum of CTD.....	S12
7. AIE Investigation of CTD.....	S12
8. Fluorescence quantum yields of nanoparticles	S13
9. Fluorescence lifetimes of nanoparticles.....	S14
10. Energy transfer efficiency	S21
11. Antenna effect (AE) calculation	S22
12. Photocatalytic cross-coupling dehydrogenation reaction	S23
13. References.....	S32

1. General information

All reactions were performed in air atmosphere unless otherwise stated. The commercially available reagents and solvents were either employed as purchased or dried according to procedures described in the literatures. Ultrapure water (pH = 6.9) was used in this work. Column chromatography was performed with silica gel (200 – 300 mesh) produced by Qingdao Marine Chemical Factory, Qingdao (China). All yields were given as isolated yields. NMR spectra were recorded on a Bruker 400 MHz spectrometer with internal standard tetramethylsilane (TMS) and solvent signals as internal references at room temperature, and the chemical shifts (δ) were expressed in ppm and J values were given in Hz. High-resolution electrospray ionization mass spectra (HR-ESI-MS) were recorded on an Agilent 6540Q-TOF LCMS equipped with an electrospray ionization (ESI) probe operating in the positive-ion mode with direct infusion. Transmission electron microscope (TEM) was carried out on a HITACHI HT-7700 instrument. Scanning electron microscope (SEM) investigations were carried out on a HITACHI SU8060 instrument. Dynamic light scattering (DLS) and Zeta-potential measurements were carried out on a computer-controlled laser diffraction apparatus (Zetasizer Nano-ZS90, Malvern Instruments Ltd., Worcestershire, UK). The UV-Vis absorption spectra were measured on a Perkin Elmer Lambda 35 UV-Vis Spectrometer. The emission spectra were recorded on a Hitachi F-7000 Fluorescence Spectrometer. The fluorescence lifetimes were measured employing time correlated single photon counting on a FS5 instrument (Edinburg Instruments Ltd., Livingstone, UK). The fluorescence quantum yields were carried out on a FS5 instrument with the integrating sphere. The pH value was tested by pH meter (FE28-standard METTLER TOLEDO). Hydrogen gas was detected by GC on a TCD analyzer (Nexis GC-2030, SHIMADZU).

2. Synthesis of CTD and CTDCG



Scheme S1. Synthesis route of CTD and CTDCG.

Synthesis of compound CTD

Compound **1** was synthesized according to previous literatures.^{S1,S2}

After synthesis of compound **1**, compound **1** (300 mg, 0.85 mmol) and 4-(9H-carbazol-9-yl)benzaldehyde (255 mg, 0.94 mmol) were dissolved in ethanol (25 mL). The mixture was stirred for 24 h and the precipitation was gradually observed. Then, the solid was obtained by centrifuge with 3000 rpm and further washed by diethyl ether (50 mL). The solid was dried at 60 °C for 8 h to afford compound **2** as a white product (462 mg, 0.77 mmol, 90%). ¹H NMR (400 MHz, CDCl₃, 298 K) δ (ppm): 8.14 (dd, *J* = 18, 7.6 Hz, 4H), 7.70 (dd, *J* = 13.6, 8.4 Hz, 4H), 7.51 (d, *J* = 6.8 Hz, 3H), 7.44 (t, *J* = 8 Hz, 2H), 7.33 (t, *J* = 7.6 Hz, 2H), 6.99 (d, *J* = 8.8 Hz, 2H), 4.03 (t, *J* = 6.4 Hz, 2H), 3.43 (t, *J* = 6.8 Hz, 2H), 1.90 – 1.78 (m, 4H), 1.51 – 1.32 (m, 12H). ¹³C NMR (100 MHz, CDCl₃, 298 K) δ (ppm): 160.2, 140.3, 139.1, 138.6, 132.7, 130.6, 127.3, 126.9, 126.5, 126.1, 123.7, 120.4, 118.2, 115.0, 111.7, 109.8, 68.2, 34.1, 32.8, 29.4, 29.3, 29.3, 29.1, 28.7, 28.1, 26.0. HR-ESI-MS: *m/z* [M + H]⁺ calcd for [C₃₇H₃₈BrN₂O]⁺ 605.2162, 607.2142, found 605.2152, 607.2133.

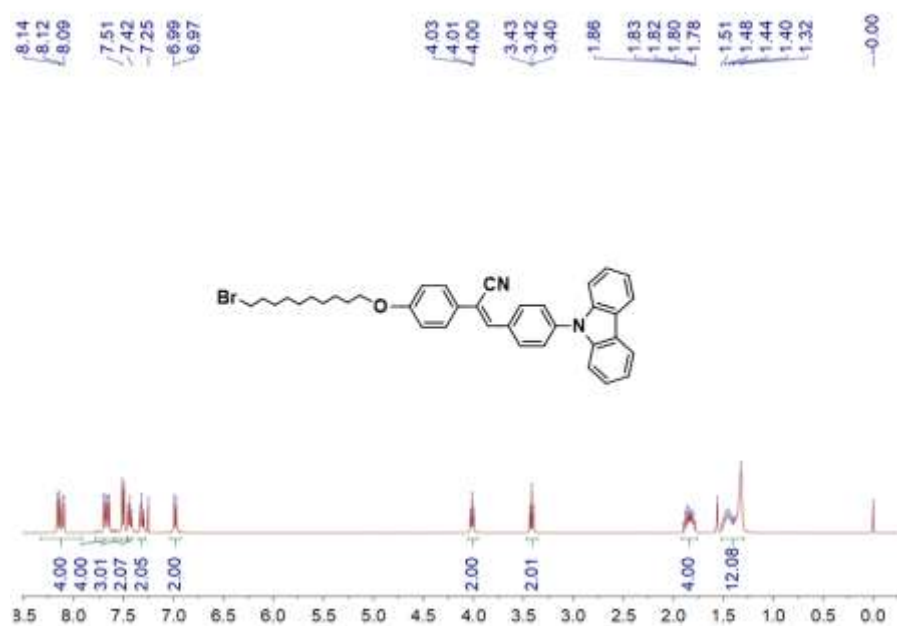


Fig. S1 ¹H NMR spectrum (400 MHz, CDCl₃, 298 K) of compound **2**.

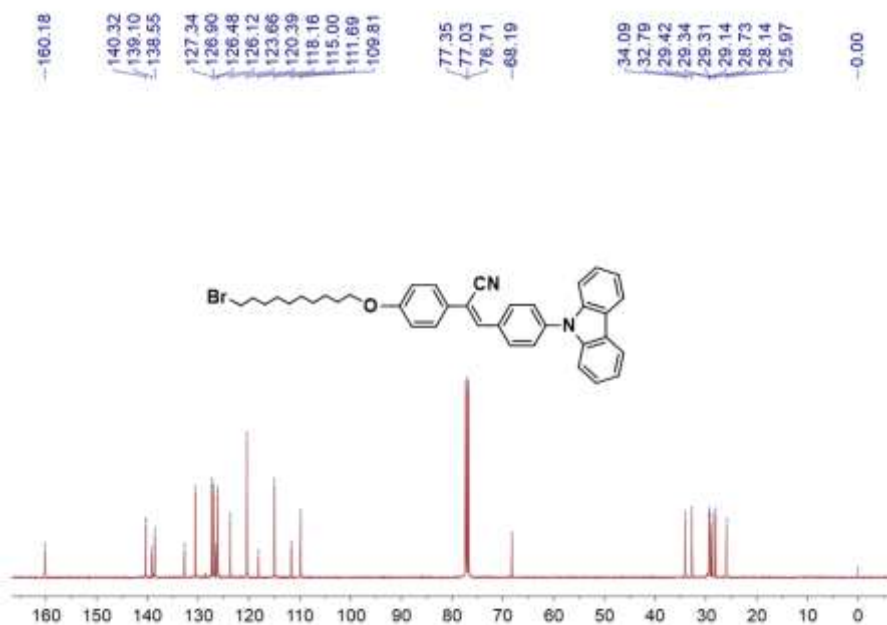


Fig. S2 ^{13}C NMR spectrum (100 MHz, CDCl_3 , 298 K) of compound 2.

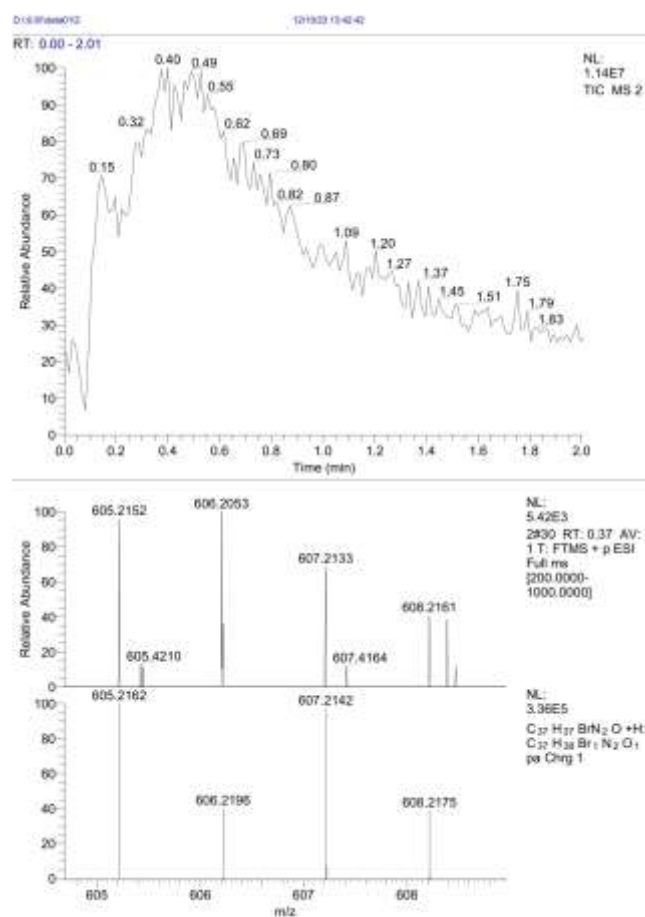


Fig. S3 HR-ESI-MS spectrum of compound 2.

Compound 2 (400 mg, 0.66 mmol) and trimethylamine solution (2.0 mL, 2 M in THF) were dissolved in ethyl acetate (EA, 20 mL). The mixture was stirred for 72 h and the yellow solid was

gradually observed. Then, the solid was separated and washed by EA (60 mL). The solid was further dried at 80 °C for 12 h to afford compound **CTD** as a yellow product (418 mg, 0.63 mmol, 95%). ¹H NMR (400 MHz, DMSO-*d*₆, 298 K) δ (ppm): 8.29 (dd, *J* = 22, 8 Hz, 4H), 8.08 (s, 1H), 7.93 – 7.66 (m, 5H), 7.52 – 7.46 (m, 3H), 7.38 – 7.32 (m, 2H), 7.11 – 7.05 (m, 2H), 4.06 (t, *J* = 6.4 Hz, 2H), 3.30 – 3.26 (m, 2H), 3.05 (s, 9H), 1.76 – 1.65 (m, 4H), 1.43 – 1.42 (m, 2H), 1.31 (b, 10H). ¹³C NMR (100 MHz, DMSO-*d*₆, 298 K) δ (ppm): 160.1, 140.1, 139.8, 138.7, 133.3, 131.2, 129.5, 127.8, 127.4, 127.2, 126.9, 126.4, 123.5, 121.1, 121.0, 118.6, 115.6, 110.6, 110.3, 68.2, 65.7, 52.6, 29.4, 29.2, 29.1, 29.0, 26.2, 26.0, 22.5. HR-ESI-MS: *m/z* [M – Br]⁺ calcd for [C₄₀H₄₆N₃O]⁺ 584.3635, found 584.3619.

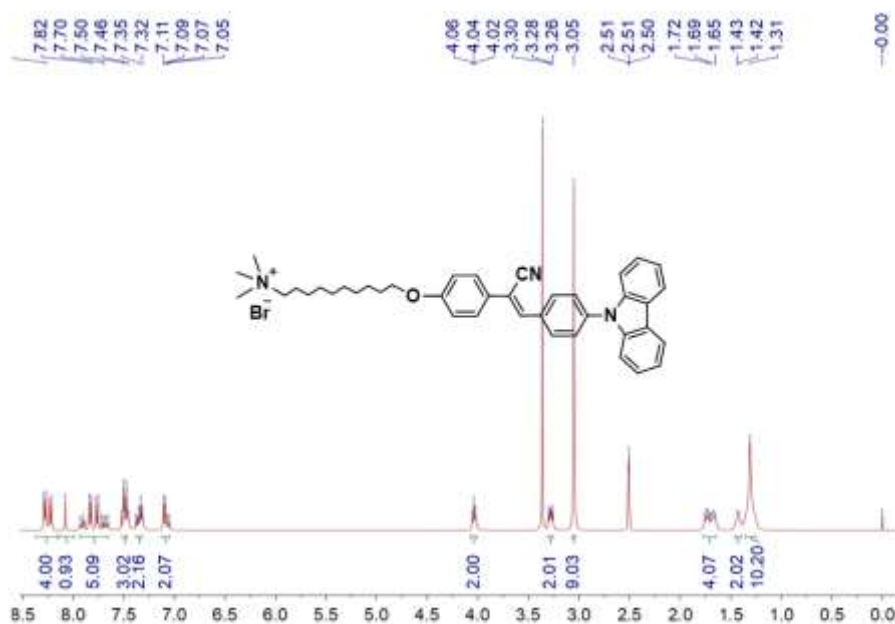


Fig. S4 ¹H NMR spectrum (400 MHz, DMSO-*d*₆, 298 K) of compound **CTD**.

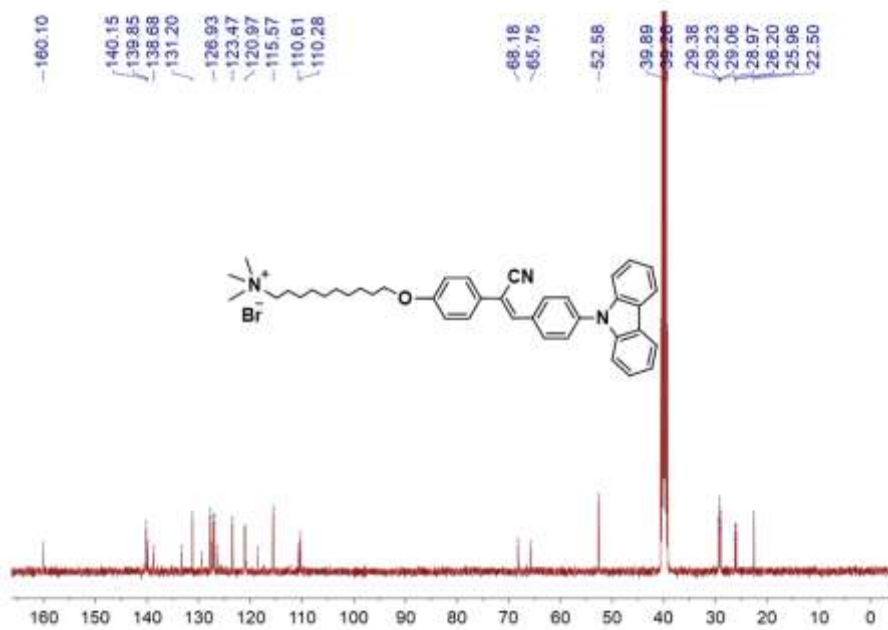


Fig. S5 ¹³C NMR spectrum (100 MHz, DMSO-*d*₆, 298 K) of compound CTD.

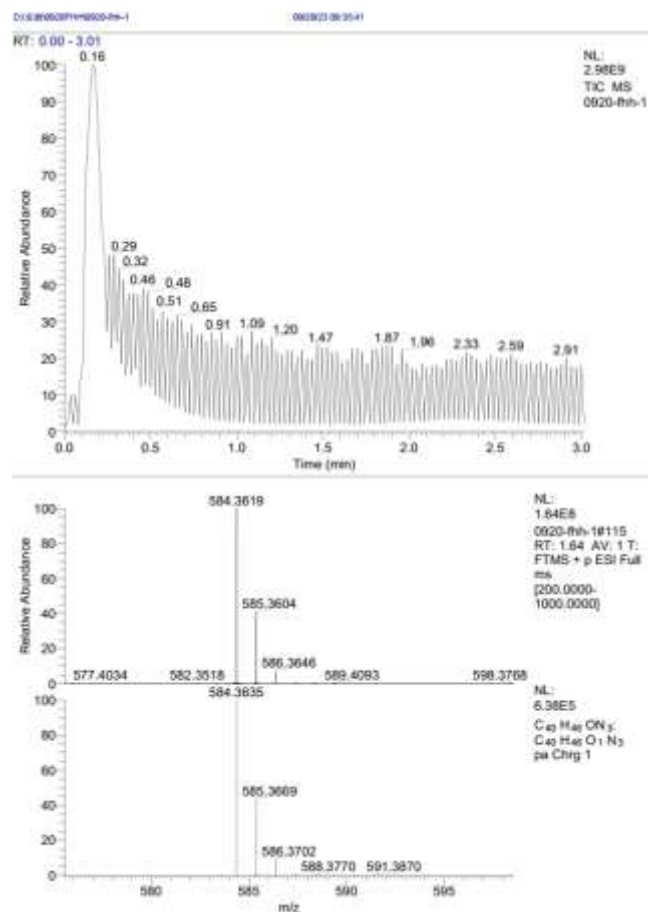


Fig. S6 HR-ESI-MS spectrum of compound CTD.

Synthesis of compound CTDCG

Compound **1** (300 mg, 0.85 mmol) and benzaldehyde (91 mg, 0.85 mmol) were firstly dissolved in ethanol (25 mL). Then, tetrabutylammonium hydroxide (TBAH, 0.5 mL) was added to the mixture and refluxed overnight under N₂ atmosphere. The reaction mixture was further concentrated and the crude product was washed by diethyl ether (60 mL) to afford compound **3** as a white solid (343 mg, 0.78 mmol, 92%). ¹H NMR (400 MHz, CDCl₃, 298 K) δ (ppm): 7.87 (d, *J* = 6.8 Hz, 2H), 7.62 – 7.59 (m, 2H), 7.48 – 7.39 (m, 4H), 6.97 – 6.93 (m, 2H), 4.02 (t, *J* = 6.8 Hz, 2H), 3.43 (t, *J* = 6.8 Hz, 2H), 1.89 – 1.77 (m, 4H), 1.49 – 1.32 (m, 12H). ¹³C NMR (100 MHz, CDCl₃, 298 K) δ (ppm): 160.0, 140.0, 134.0, 130.1, 129.1, 128.9, 127.3, 126.7, 118.2, 115.0, 111.4, 68.2, 34.1, 32.8, 29.4, 29.4, 29.3, 29.2, 28.8, 28.2, 26.0. HR-ESI-MS: *m/z* [M + H]⁺ calcd for [C₂₅H₃₁BrNO]⁺ 440.1584, 442.1563, found 440.1577, 442.1558.

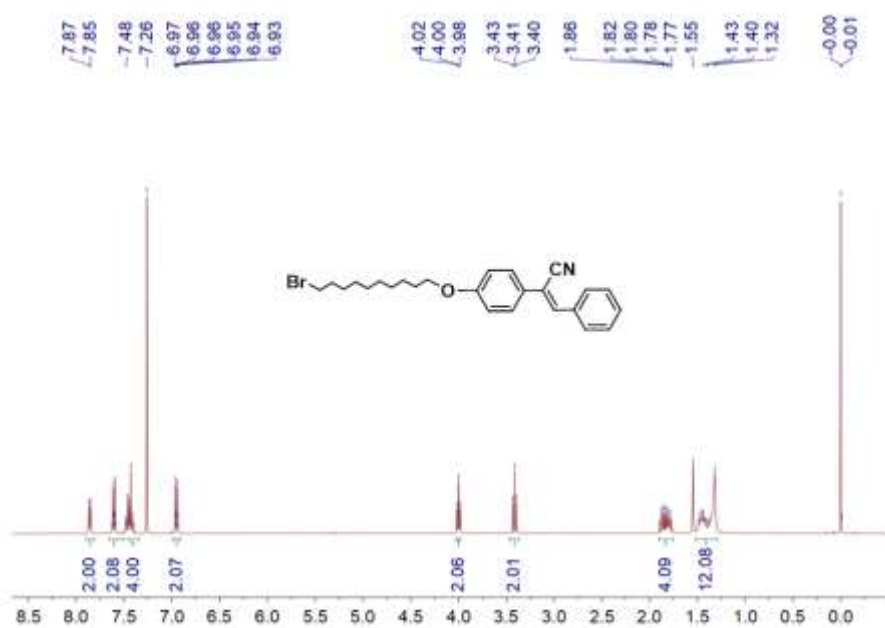


Fig. S7 ¹H NMR spectrum (400 MHz, CDCl₃, 298 K) of compound **3**.

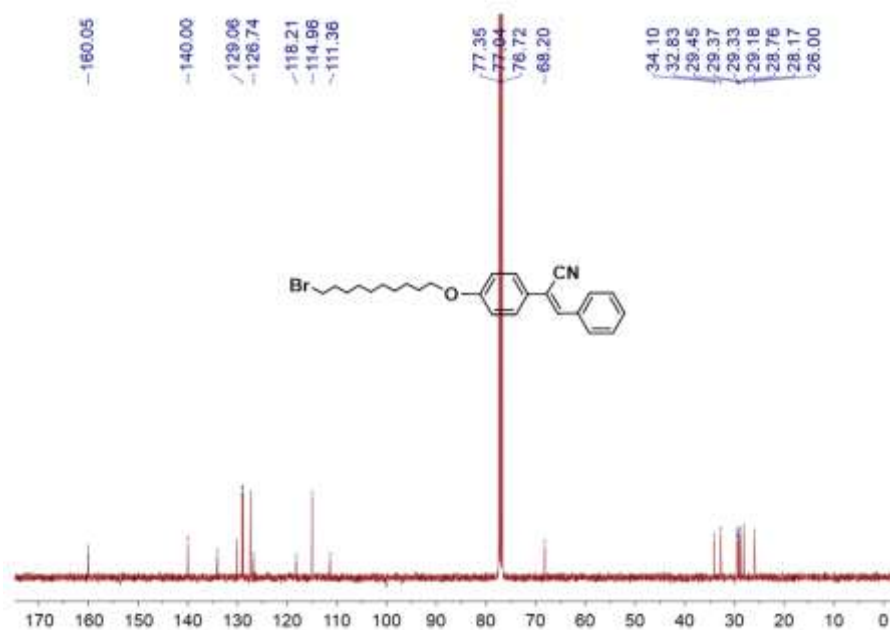


Fig. S8 ¹³C NMR spectrum (100 MHz, CDCl₃, 298 K) of compound 3.

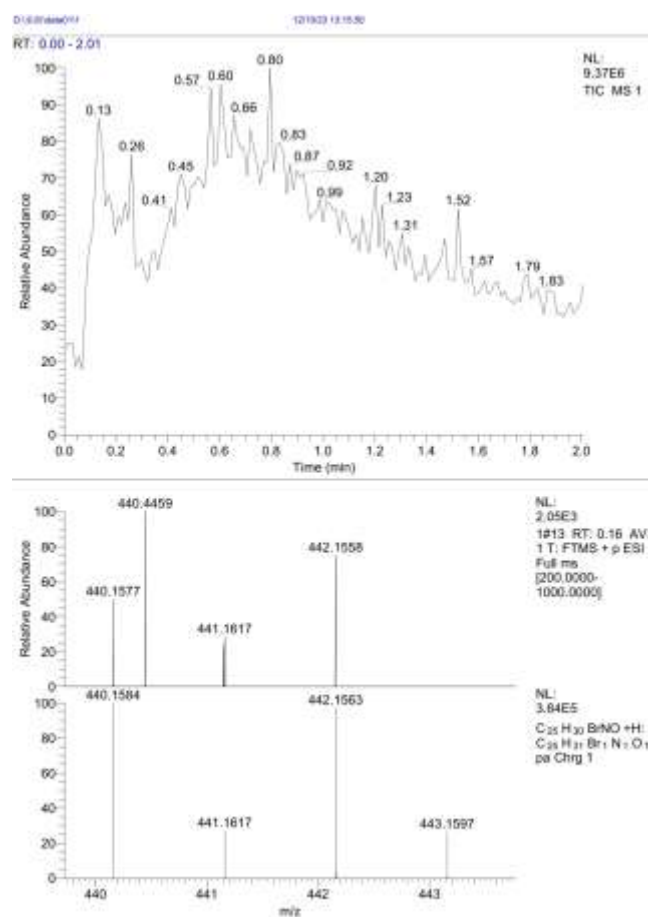


Fig. S9 HR-ESI-MS spectrum of compound 3.

Compound 3 (300 mg, 0.68 mmol) and trimethylamine solution (2.0 mL, 2 M in THF) were dissolved in CHCl₃ (20 mL). Then, the mixture was stirred and refluxed overnight under N₂

atmosphere. The reaction mixture was concentrated and the obtained solid was washed by diethyl ether (60 mL). The product was dried at 80 °C for 12 h to afford compound **CTDCG** as a yellow solid (335 mg, 0.67 mmol, 99%). ¹H NMR (400 MHz, DMSO-*d*₆, 298 K) δ (ppm): 7.93 (dd, *J* = 5.6, 4 Hz, 3H), 7.71 (d, *J* = 7.2 Hz, 2H), 7.56 – 7.46 (m, 3H), 7.08 (d, *J* = 8.8 Hz, 2H), 4.05 (t, *J* = 6.4 Hz, 2H), 3.29 – 3.24 (m, 2H), 3.04 (s, 9H), 1.77 – 1.63 (m, 4H), 1.45 – 1.24 (m, 12H). ¹³C NMR (100 MHz, DMSO-*d*₆, 298 K) δ (ppm): 159.4, 140.4, 133.9, 130.1, 128.8, 128.8, 127.1, 125.8, 117.9, 114.9, 109.8, 67.6, 65.1, 52.0, 28.8, 28.6, 28.5, 28.4, 25.6, 25.4, 21.9. HR-ESI-MS: *m/z* [M – Br]⁺ calcd for [C₂₈H₃₉N₂O]⁺ 419.3057, found 419.3049.

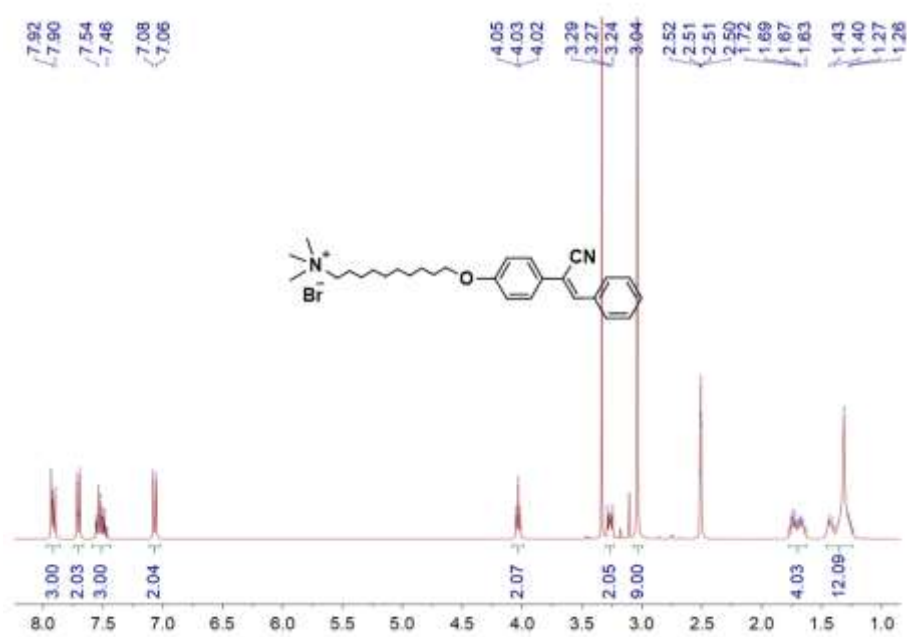


Fig. S10 ¹H NMR spectrum (400 MHz, DMSO-*d*₆, 298 K) of compound **CTDCG**.

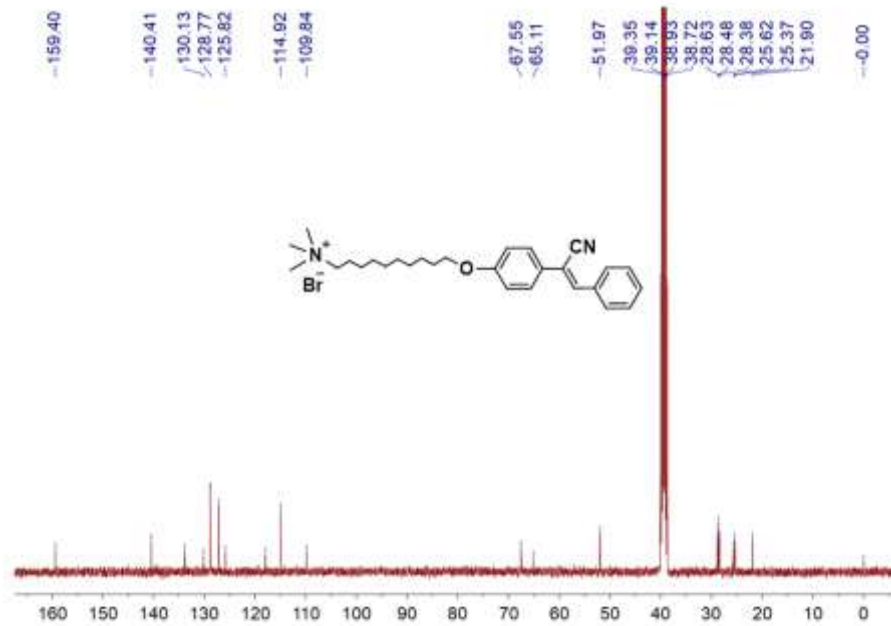


Fig. S11 ¹³C NMR spectrum (100 MHz, DMSO-*d*₆, 298 K) of compound CTDCG.

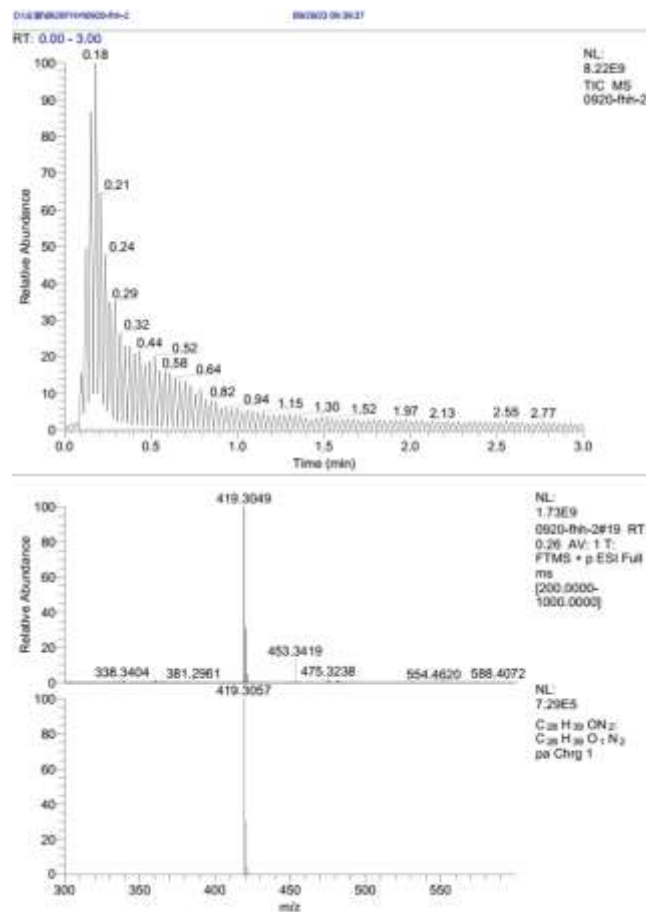


Fig. S12 HR-ESI-MS spectrum of compound CTDCG.

3. Host-guest interaction of WPP5 and CTD

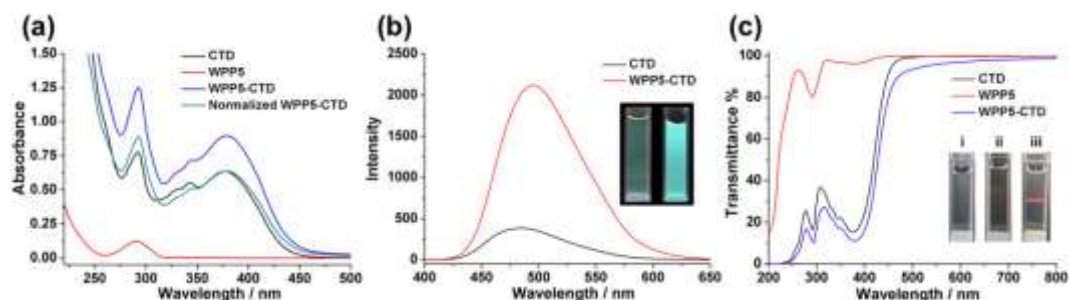


Fig. S13 (a) Absorbance spectra of CTD, WPP5, WPP5-CTD, and Normalized WPP5-CTD. (b) Fluorescence spectra of CTD and WPP5-CTD. Inset: Fluorescence photos of CTD (left) and WPP5-CTD (right). (c) Transmittance spectra of CTD, WPP5, and WPP5-CTD. Inset: Tyndall effect photos of (i) CTD, (ii) WPP5, and (iii) WPP5-CTD.

4. Fabrication of nanoparticle

After synthesis of CTD and CTDCG, WPP5-CTD, WPP5-CTD-ESY, WPP5-CTDCG, and WPP5-CTDCG-ESY nanoparticles were fabricated as follow. Firstly, CTD (0.02 M, DMSO), CTDCG (0.02 M, DMSO), WPP5 (4.2×10^{-4} M, H₂O), and ESY (2×10^{-4} M, DMSO) solution were prepared, respectively. Then, 10 μ L CTD (or CTDCG) solution and 48 μ L WPP5 solution were mixed in 4 mL water to afford WPP5-CTD (or WPP5-CTDCG) nanoparticles (pH = 6.9). 10 μ L CTD (or CTDCG) solution, 0-10 μ L ESY solution and 48 μ L WPP5 solution were mixed in 4 mL water to afford WPP5-CTD-ESY (or WPP5-CTDCG-ESY) nanoparticles (pH = 6.9).

5. Zeta potential results of WPP5-CTD and WPP5-CTD-ESY

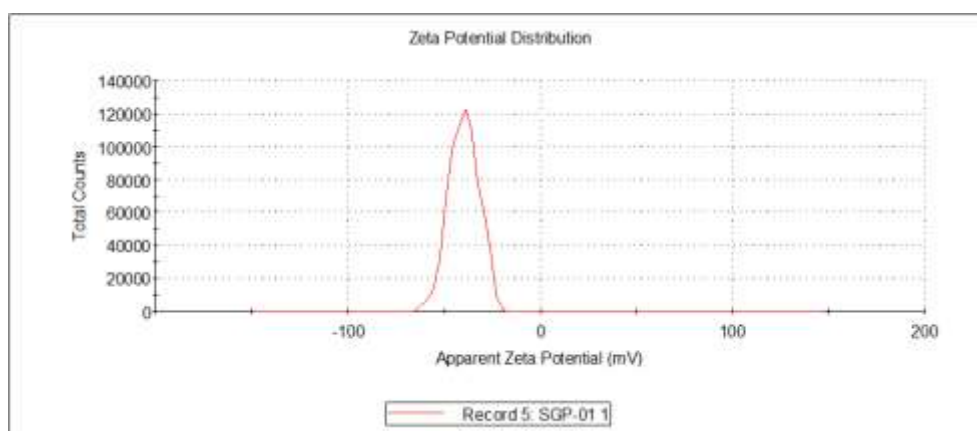


Fig. S14 Zeta potential result of WPP5-CTD solution.

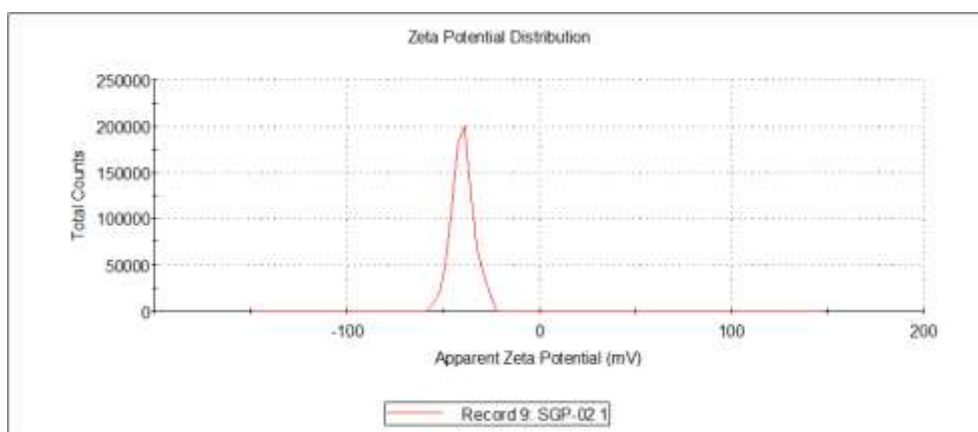


Fig. S15 Zeta potential result of WPP5-CTD-ESY solution.

6. Absorbance spectrum of CTD

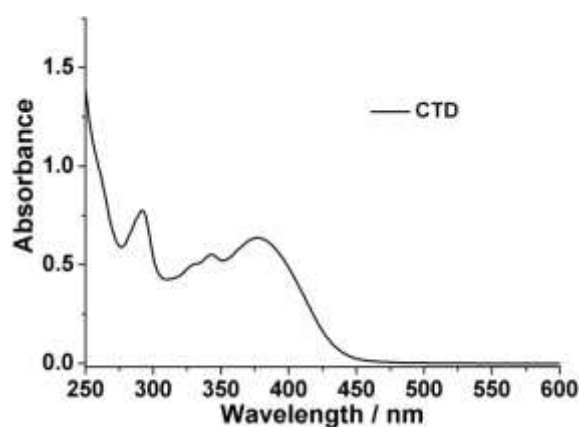


Fig. S16 Absorbance spectrum of CTD.

7. AIE Investigation of CTD

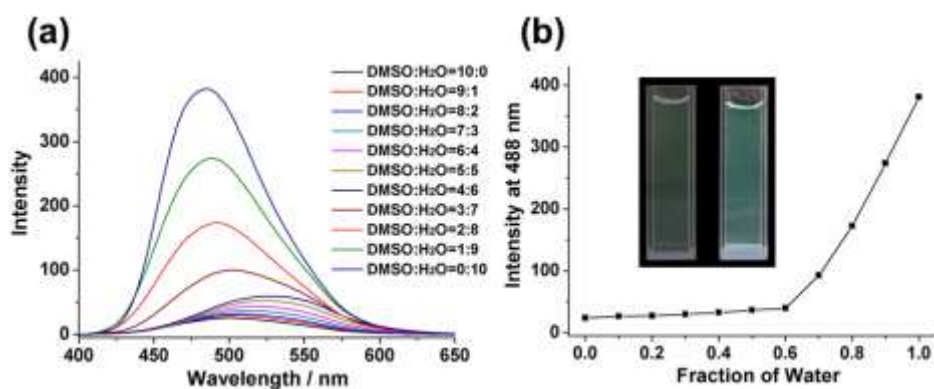


Fig. S17 (a) Fluorescence spectra of CTD (0.05 mM) in DMSO/H₂O mixed solvent under 365 nm excitation. (b) The fluorescent intensity change of CTD at 488 nm with different volume percentage of water from 0 to 100%. Inset: Fluorescence photos of 0 (left) and 100% (right).

8. Fluorescence quantum yields of nanoparticles

According to the reported literature,^{S3} the absolute quantum yield could be obtained by the equation of “ $\Phi = (\text{number of photons emitted}) / (\text{number of photons absorbed})$ ”. In the integrating sphere method of FS5, “the number of photons emitted” is calculated by choosing the “Emission Range” and “the number of photons absorbed” is calculated by choosing the “Scatter Range”.

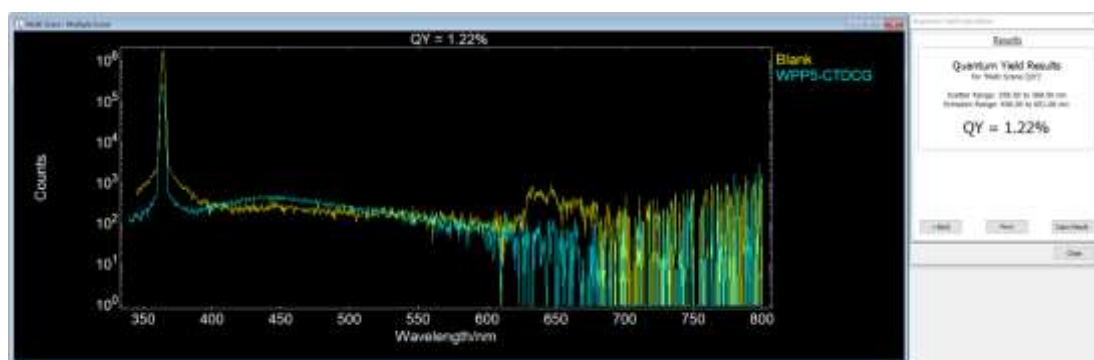


Fig. S18 The absolute fluorescence quantum yield of **WPP5-CTDCG** nanoparticle under 365 nm excitation. Scatter Range: 359.5 nm to 368.5 nm; Emission Range: 406 nm to 601 nm.

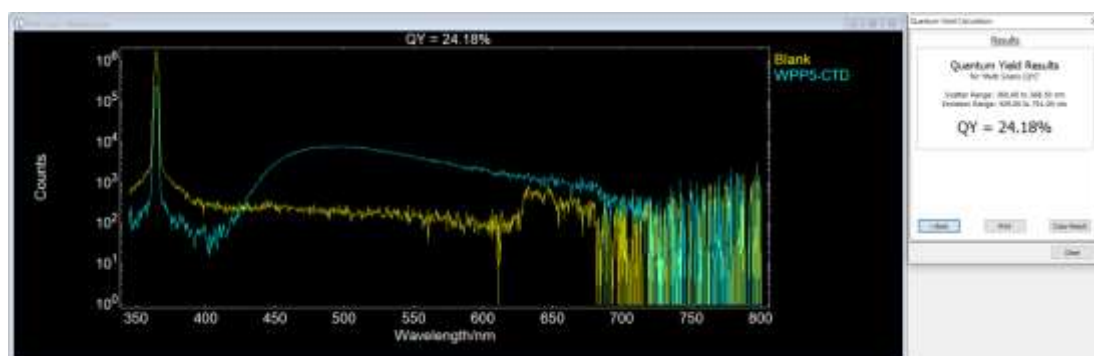


Fig. S19 The absolute fluorescence quantum yield of **WPP5-CTD** nanoparticle under 365 nm excitation. Scatter Range: 360 nm to 368.5 nm; Emission Range: 429 nm to 701 nm.

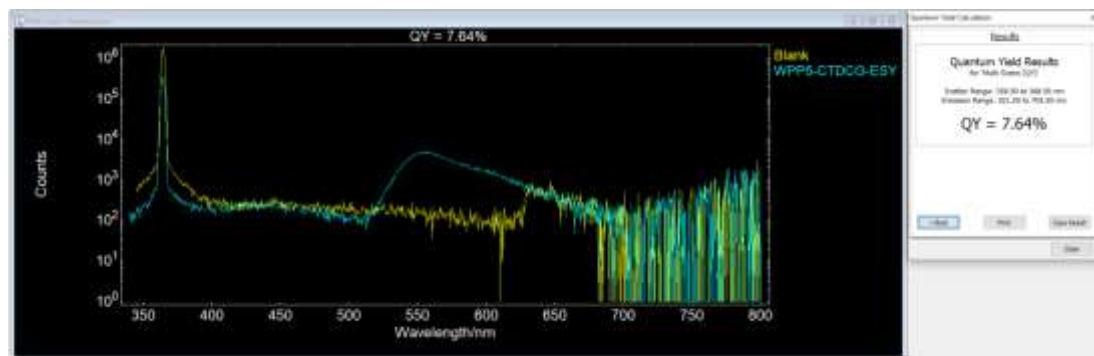


Fig. S20 The absolute fluorescence quantum yield of **WPP5-CTDCG-ESY** nanoparticle under 365 nm excitation. Scatter Range: 359.5 nm to 368.5 nm; Emission Range: 521 nm to 705.5 nm.

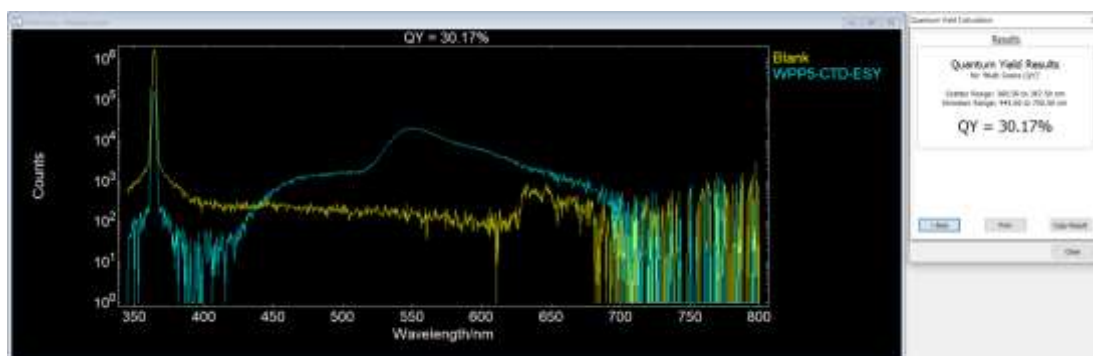


Fig. S21 The absolute fluorescence quantum yield of **WPP5-CTD-ESY** nanoparticle under 365 nm excitation. Scatter Range: 360.5 nm to 367.5 nm; Emission Range: 445 nm to 700.5 nm.

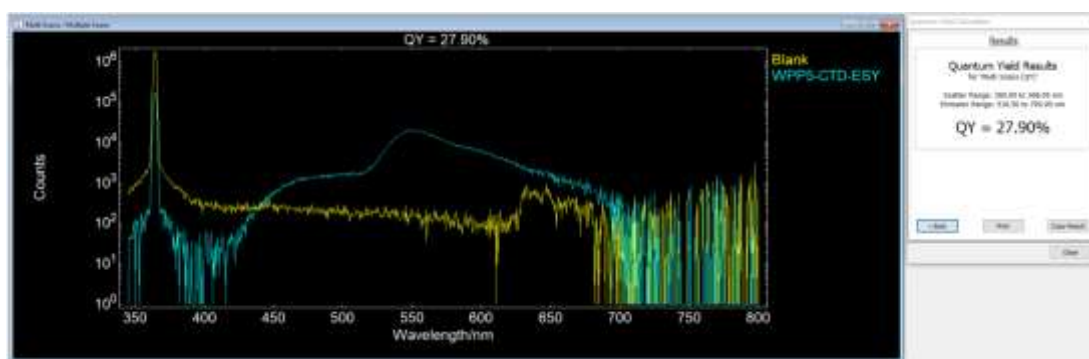


Fig. S22 The absolute fluorescence quantum yield of **ESY** part in **WPP5-CTD-ESY** nanoparticle under 365 nm excitation. Scatter Range: 360 nm to 368 nm; Emission Range: 516.5 nm to 700 nm.

9. Fluorescence lifetimes of nanoparticles

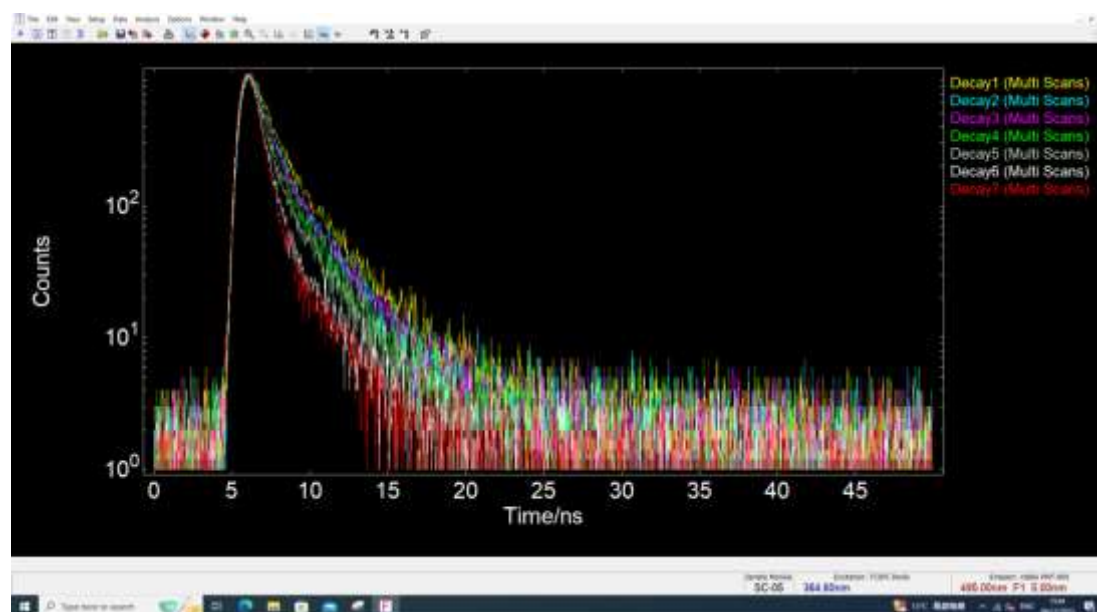


Fig. S23 Fluorescence decay curves of **WPP5-CTD** (Decay1) and **WPP5-CTD-ESY** at different

molar ratios of CTD:ESY (2000:1 (Decay2), 1000:1 (Decay3), 500:1 (Decay4), 350:1 (Decay5), 250:1 (Decay6), and 200:1 (Decay7)) monitored at 495 nm under 365 nm excitation.

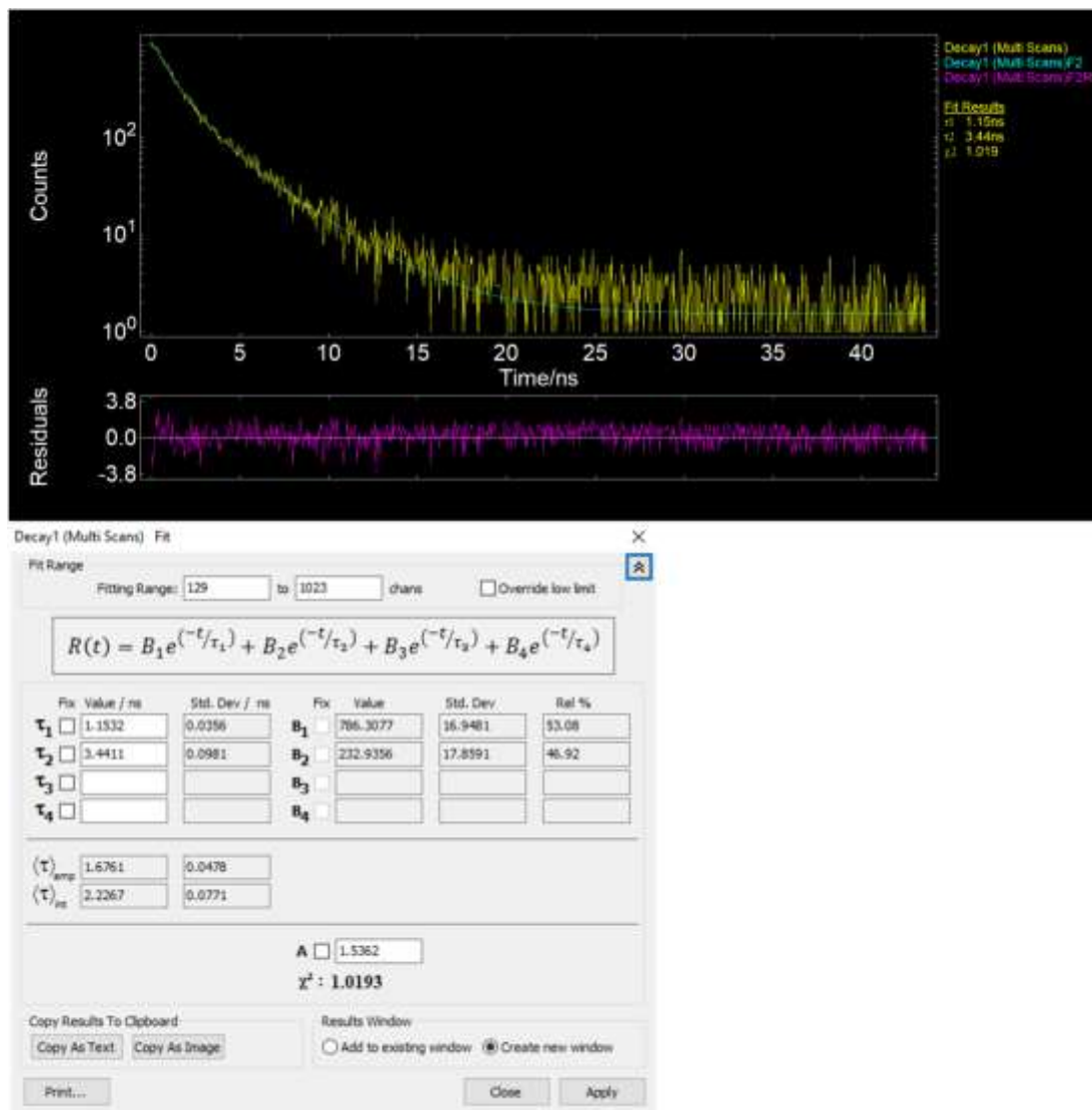


Fig. S24 Fluorescence decay curve and lifetime of WPP5-CTD (Decay1) monitored at 495 nm under 365 nm excitation.

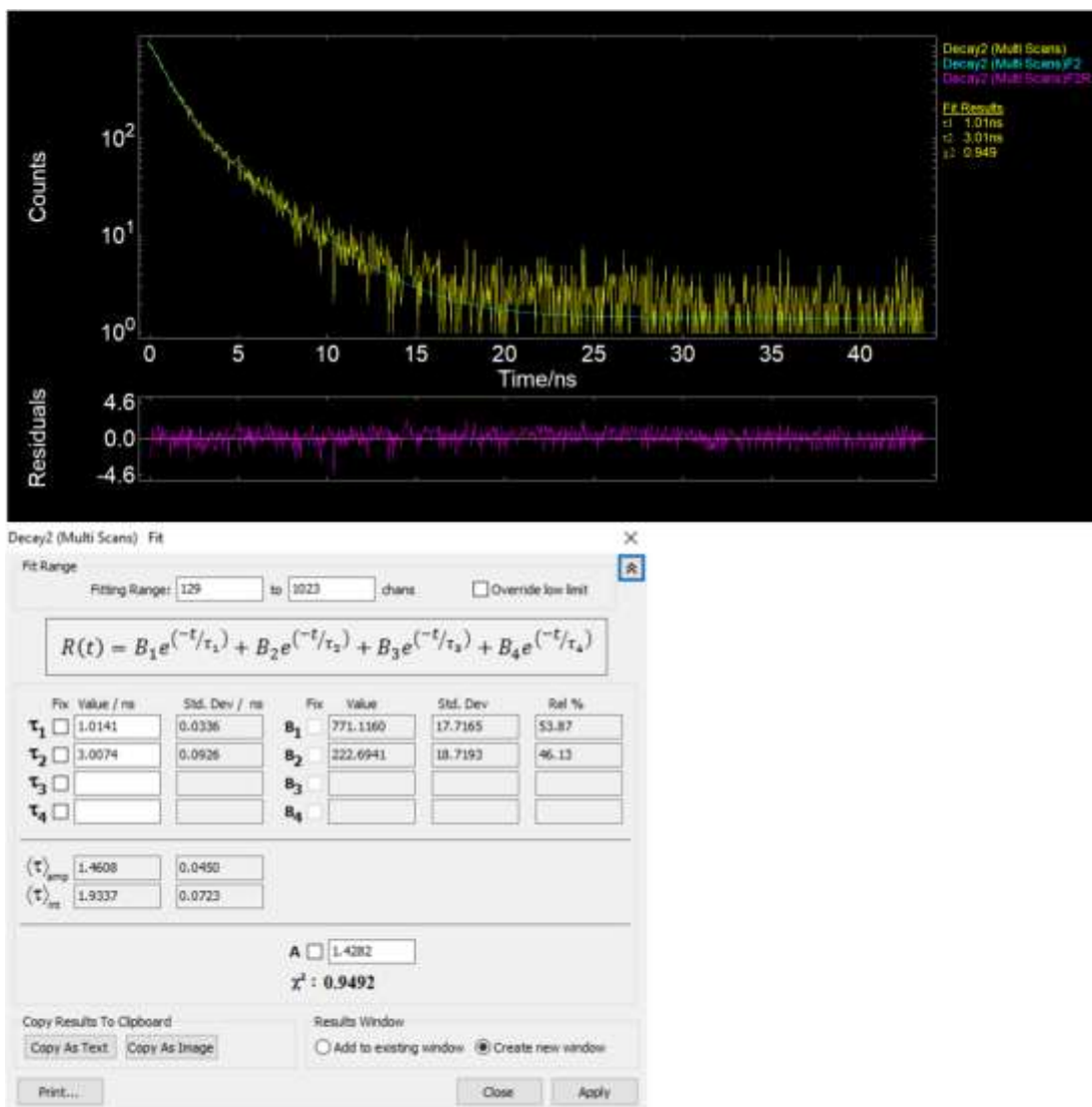


Fig. S25 Fluorescence decay curve and lifetime of WPP5-CTD-ESY at the molar ratio of CTD:ESY (2000:1 (Decay2)) monitored at 495 nm under 365 nm excitation.

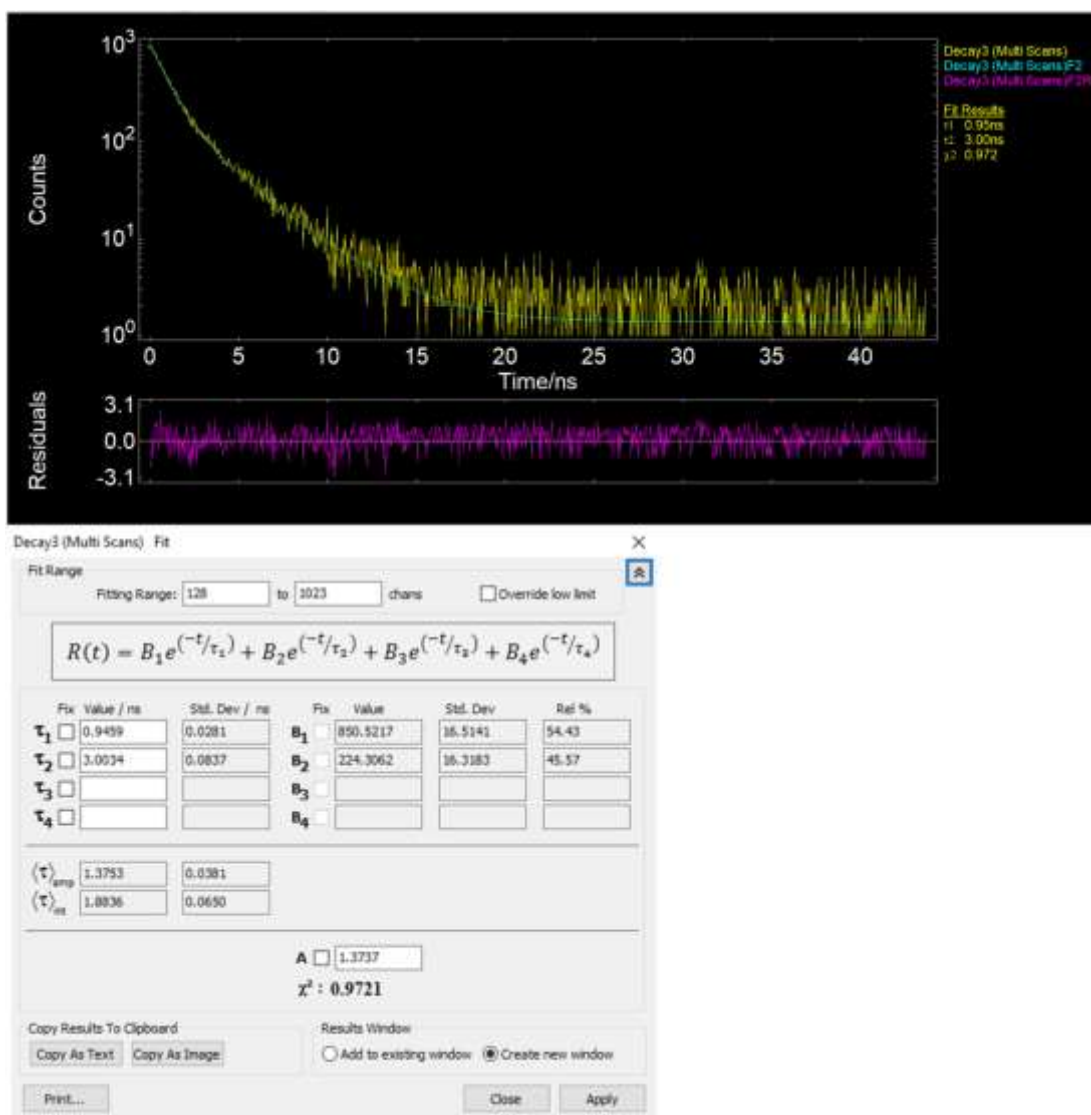


Fig. S26 Fluorescence decay curve and lifetime of **WPP5-CTD-ESY** at the molar ratio of **CTD:ESY** (1000:1 (Decay3)) monitored at 495 nm under 365 nm excitation.

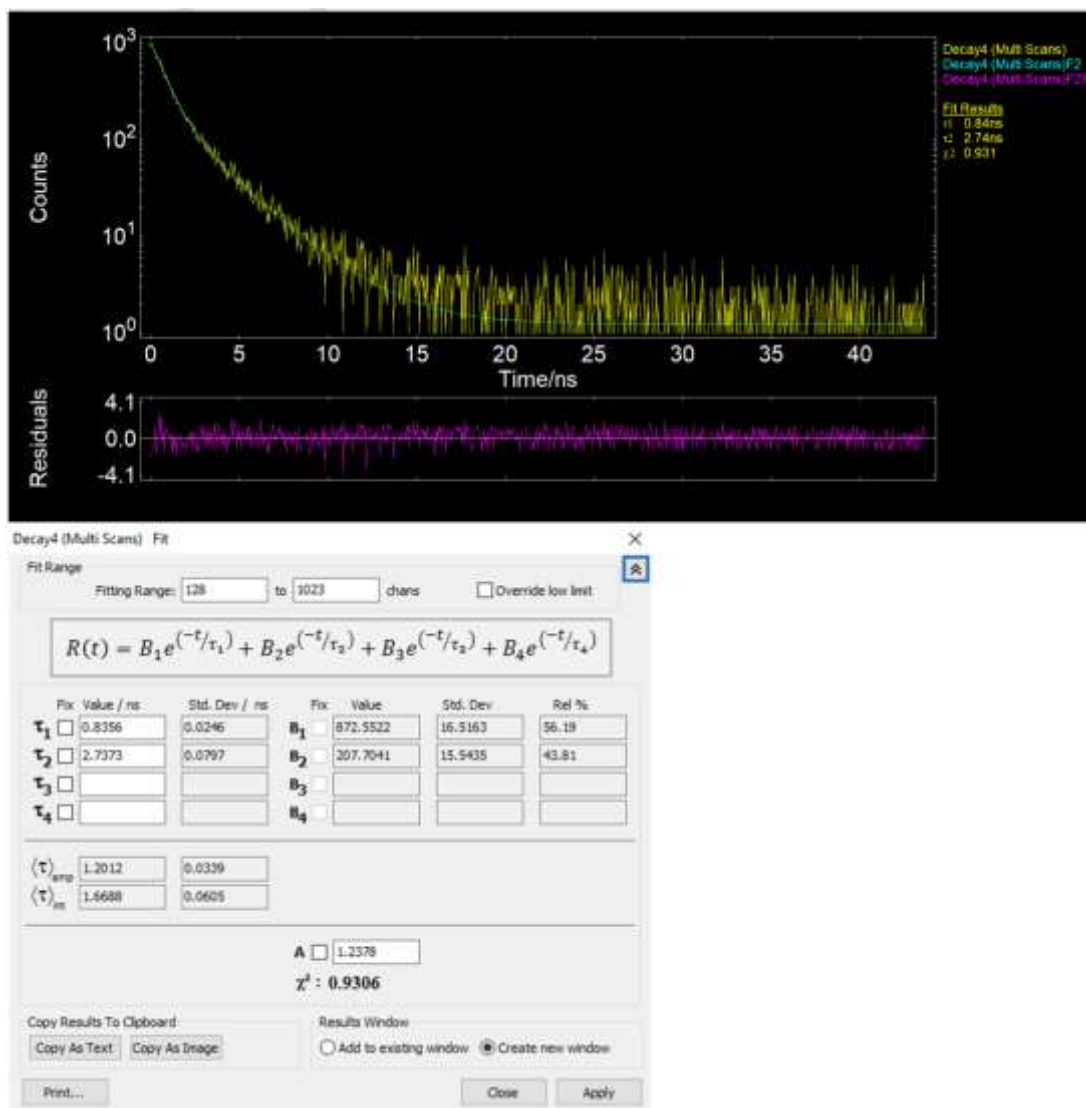


Fig. S27 Fluorescence decay curve and lifetime of WPP5-CTD-ESY at the molar ratio of CTD:ESY (500:1 (Decay4)) monitored at 495 nm under 365 nm excitation.

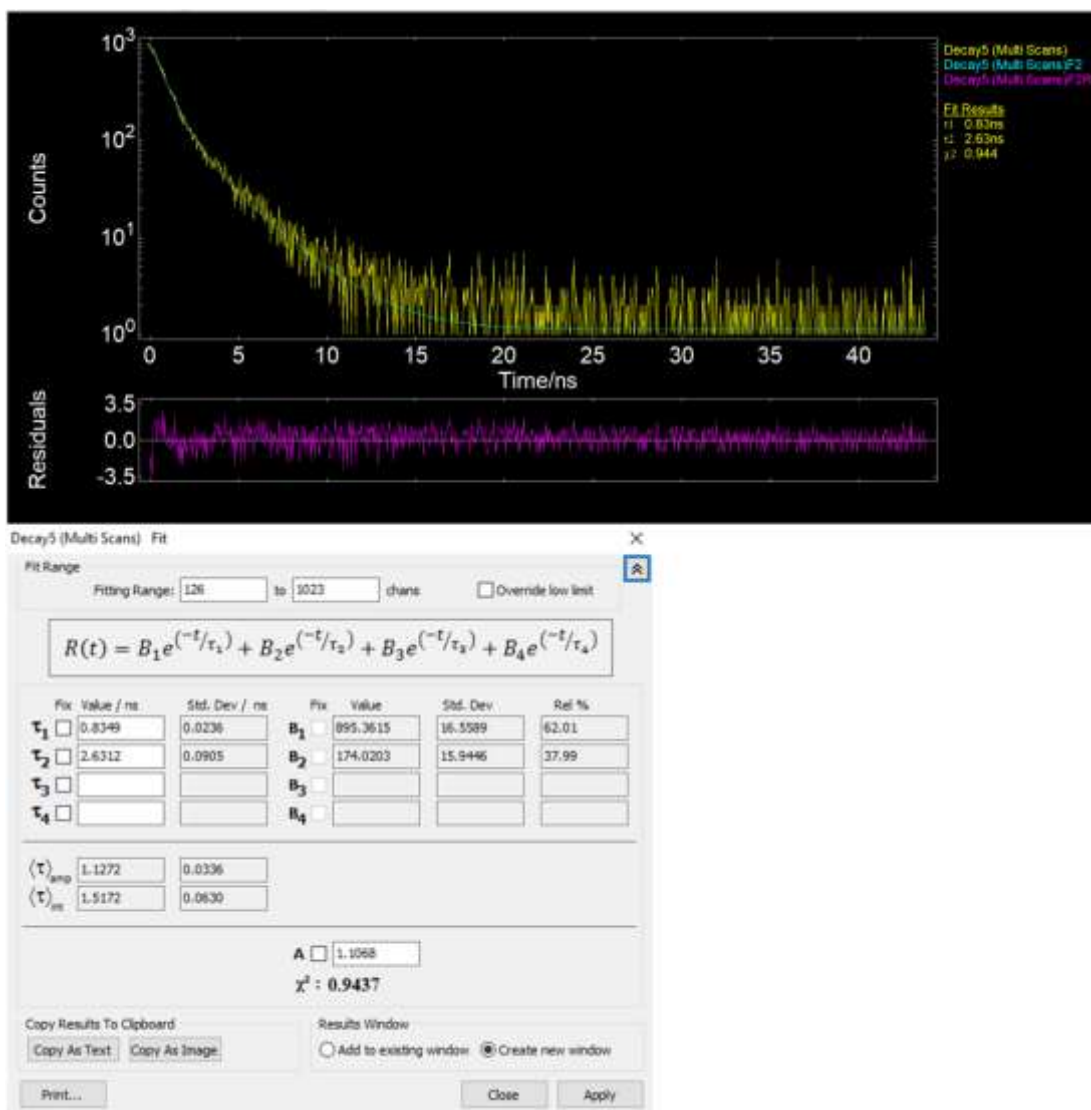


Fig. S28 Fluorescence decay curve and lifetime of **WPP5-CTD-ESY** at the molar ratio of **CTD:ESY (350:1 (Decay5))** monitored at 495 nm under 365 nm excitation.

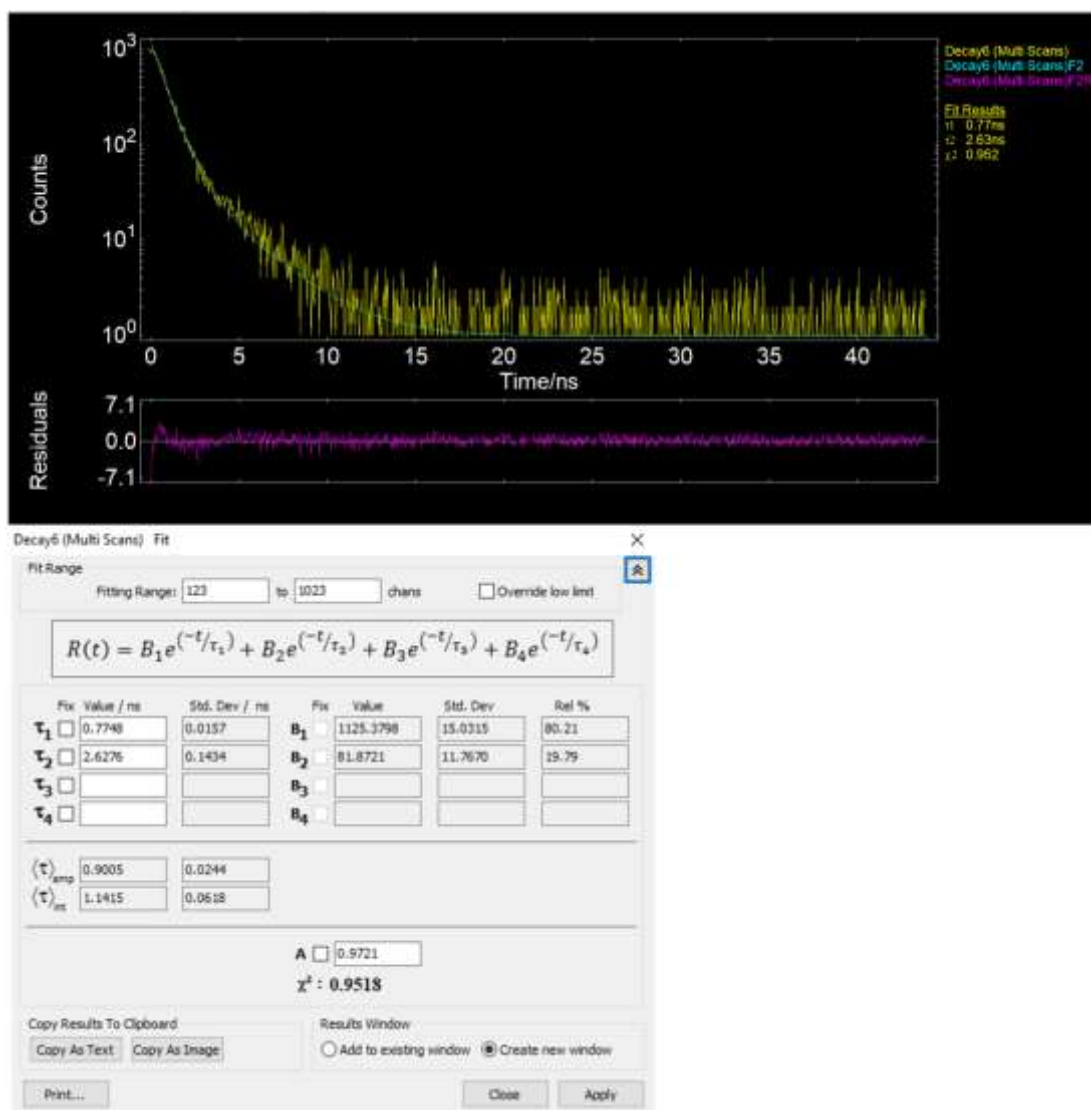


Fig. S29 Fluorescence decay curve and lifetime of **WPP5-CTD-ESY** at the molar ratio of **CTD:ESY (250:1 (Decay6))** monitored at 495 nm under 365 nm excitation.

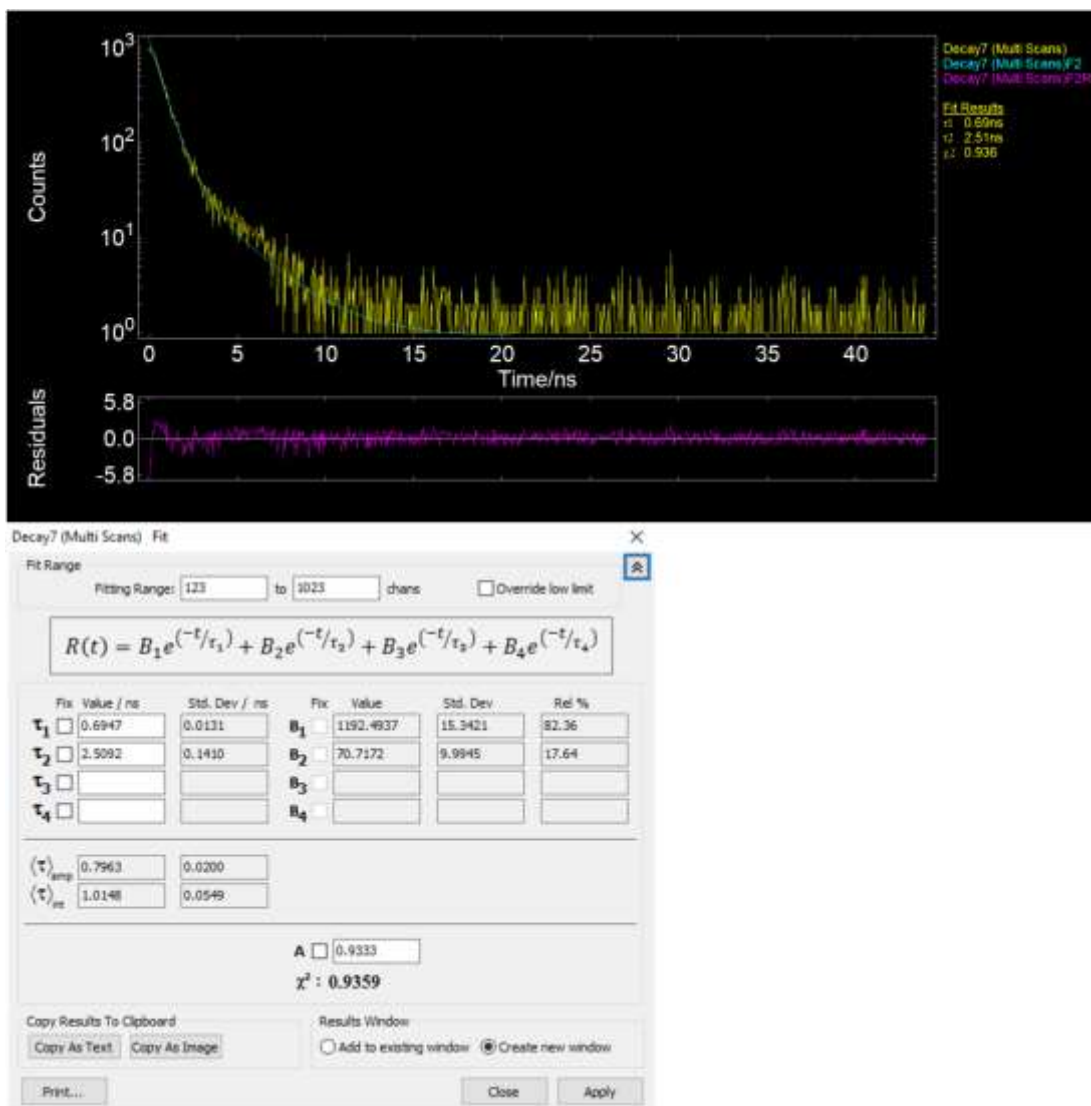


Fig. S30 Fluorescence decay curve and lifetime of **WPP5-CTD-ESY** at the molar ratio of **CTD:ESY** (200:1 (Decay7)) monitored at 495 nm under 365 nm excitation.

10. Energy transfer efficiency

The energy transfer efficiency (Φ_{ET}) was calculated according to the equation of “ $\Phi_{ET} = 1 - I_{DA} / I_D$ ”, where I_{DA} and I_D are the fluorescence intensities of **WPP5-CTD-ESY** and **WPP5-CTD** at 495 nm under 365 nm excitation.

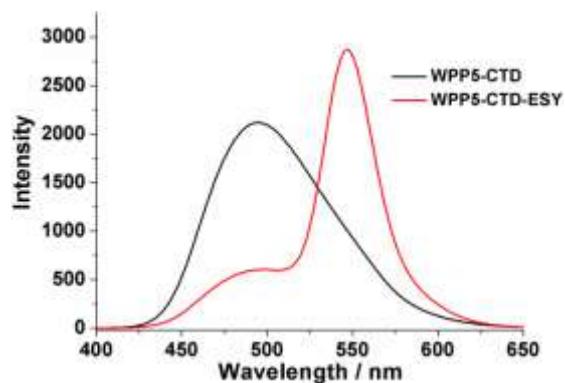


Fig. S31 Fluorescence spectra of **WPP5-CTD** and **WPP5-CTD-ESY** under 365 nm excitation. [CTD] = 5×10^{-5} M and [ESY] = 2.5×10^{-7} M, respectively.

According to the intensity of supramolecular nanoparticles at 495 nm, the energy transfer efficiency (Φ_{ET}) of **WPP5-CTD-ESY** was calculated to be 72.8% in water.

11. Antenna effect (AE) calculation

The antenna effect (AE) was calculated according to the equation of “ $AE = (I_{DA,365} - I_{D,365}) / I_{DA,500}$ ”, where $I_{DA,365}$ and $I_{DA,500}$ are the fluorescence intensities of **WPP5-CTD-ESY** at 546 nm with the excitation of the donor (CTD) at 365 nm and the direct excitation of the acceptor (ESY) at 500 nm, respectively. $I_{D,365}$ is the fluorescence intensity of **WPP5-CTD** at 546 nm, which was normalized with **WPP5-CTD-ESY** at 495 nm.

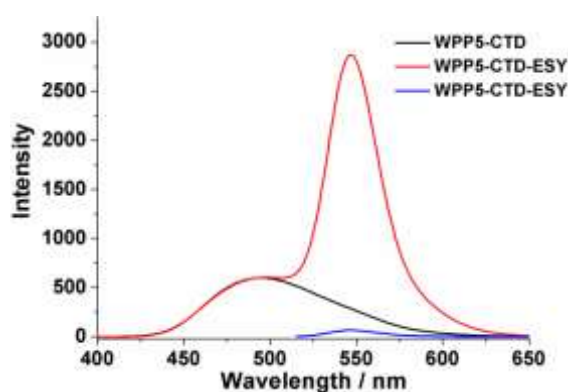


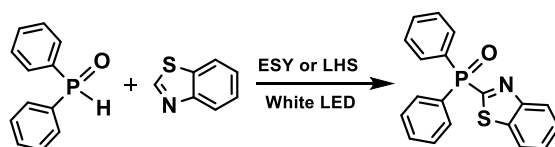
Fig. S32 Fluorescence spectrum of **WPP5-CTD** (black line), which was normalized with **WPP5-CTD-ESY** (red line) at 495 nm; Fluorescence spectra of **WPP5-CTD-ESY** (red line under 365 nm excitation and blue line under 500 nm excitation). [CTD] = 5×10^{-5} M and [ESY] = 2.5×10^{-7} M, respectively.

According to the intensity of supramolecular nanoparticles at 546 nm, the antenna effect of **WPP5-CTD-ESY** was calculated to be 38.5 in water.

Table S1. Energy transfer efficiency and antenna effect with different molar ratios of **CTD** and **ESY**.

Sample	Energy transfer efficiency	Antenna effect
CTD:ESY = 200:1	72.8%	38.5
CTD:ESY = 250:1	55.7%	40.4
CTD:ESY = 350:1	43.3%	42
CTD:ESY = 500:1	30.3%	43
CTD:ESY = 1000:1	10.6%	42.5
CTD:ESY = 2000:1	3.8%	41.5

12. Photocatalytic cross-coupling dehydrogenation reaction

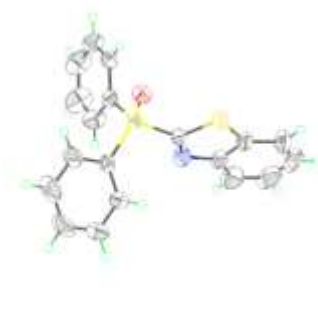


Scheme S2. Photocatalytic cross-coupling dehydrogenation reaction.

According to previous literatures,^{S4-S6} supramolecular nanoparticles were prepared according to the above experimental procedures, respectively. Benzothiazole (10 μmol , 1 equiv.) and diphenylphosphine oxide (40 μmol , 4 equiv.) were added in the freshly prepared LHS or Eosin Y (ESY) solution (4 mL) in a 10 mL glass vial. The mixture was cooled by liquid nitrogen and degassed with nitrogen for three times, and then irradiated by 11 W White LED at room temperature for corresponding time. After that, the mixture was extracted with 20 mL ethyl acetate and the combined organic layer was washed with saturated NaHCO_3 solution and brine. The solvent was removed to afford product and the crystal structure of product was successfully obtained (Fig. S33 and S34).

Table S2. Crystal data and structure refinement for the photocatalytic product.

CCDC number	2305323
Empirical formula	C ₁₉ H ₁₄ NOPS
Formula weight	335.34
Temperature / K	296.15
Crystal system	triclinic
Space group	P-1
Unit cell dimensions	a = 8.385(2) Å, b = 10.473(3) Å, c = 10.511(3) Å $\alpha = 109.339(3)^\circ$, $\beta = 92.044(3)^\circ$, $\gamma = 92.044(3)^\circ$
Volume/Å ³	843.6(4)
Z	2
$\rho_{\text{calc}} / \text{g}\cdot\text{cm}^{-3}$	1.320
μ / mm^{-1}	0.290
F(000)	348.0
Crystal size / mm ³	0.25 × 0.22 × 0.21
Radiation	MoK α ($\lambda = 0.71073$ Å)
2 θ range for data collection / °	5.724 to 55.062
Index ranges	-10 ≤ h ≤ 10, -13 ≤ k ≤ 13, -13 ≤ l ≤ 13
Reflections collected	24318
Independent reflections	3858 [$R_{\text{int}} = 0.0209$, $R_{\text{sigma}} = 0.0108$]
Data / restraints / parameters	3858 / 0 / 209
Goodness-of-fit on F ²	1.065
Completeness to theta = 27.531°	99.3%
Refinement method	Full-matrix least-squares on F ²
Final R indexes [$I \geq 2\sigma(I)$]	$R_1 = 0.0333$, $wR_2 = 0.0858$
Final R indexes [all data]	$R_1 = 0.0366$, $wR_2 = 0.0896$
Largest diff. peak / hole / e.Å ⁻³	0.34 and -0.38

**Fig. S33** X-ray Structure of the photocatalytic product. Thermal ellipsoids were shown at 50% probability level.

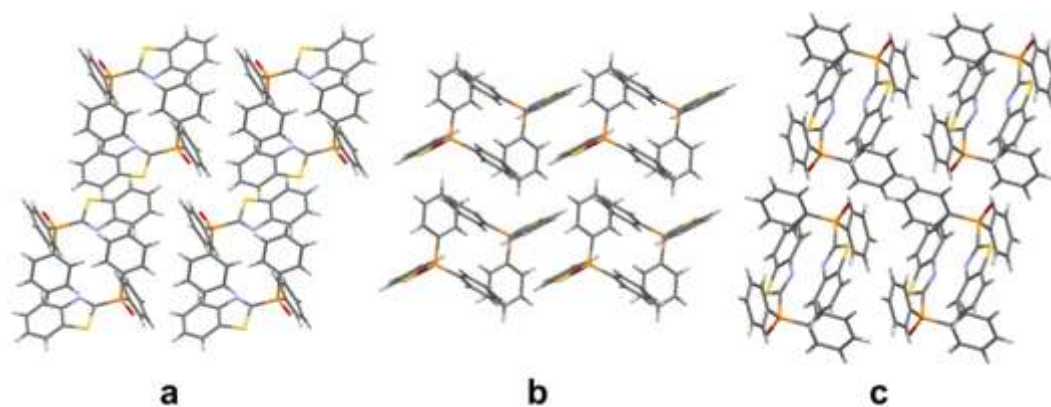


Fig. S34 The crystal packing of product viewed along a, b, and c axes.

In order to further investigate the quantum yield of the photocatalytic reaction, a quantum yield measurement was carried out.^{S7,S8} Initially, a ferrioxalate actinometry solution was prepared by following the Hammond variation of the Hatchard and Parker procedure outlined in Handbook of Photochemistry. Ferrioxalate actinometer solution measures the decomposition of ferric ions to ferrous ions, which are complexed by 1,10-phenanthroline and monitored by UV-Vis absorbance at 510 nm. The moles of iron-phenanthroline complex formed are related to moles of photons absorbed.

The solutions were prepared and stored in the dark (red light):

- 1) Potassium ferrioxalate solution: 294.8 mg of potassium ferrioxalate (commercially available from Alfa Aesar) and 139 μL of sulfuric acid (96%) were added to a 50 mL volumetric flask, and filled to the mark with water (HPLC grade).
- 2) Phenanthroline solution: 0.2% by weight of 1,10-phenanthroline in water (100 mg in 50 mL volumetric flask).
- 3) Buffer solution: to a 50 mL volumetric flask 4.94 g of NaOAc and 0.5 mL of sulfuric acid (96%) were added and filled to the mark with water (HPLC grade).
- 4) Model reaction solution: benzothiazole (10 μmol), diphenylphosphine oxide (40 μmol), Eosin Y (0.001 μmol) in the water (0.5 mL) was irradiated by White LED.

The actinometry measurements were done as follows:

- 1) 0.5 mL of the actinometer solution was added to a quartz cuvette ($l = 10$ mm). The cuvette was placed along with a sample solution (0.5 mL in a similar cuvette) whose quantum yield has to be measured (our model reaction). The sample and actinometry solutions (placed 10 cm away from the lamp) were irradiated with 11 W White LED for specified time intervals (0, 30, 60, 90, 120,

180, 210) seconds.

2) After irradiation all the actinometer solution was removed and placed in a 10 mL volumetric flask. 0.5mL of 1,10-phenanthroline solution and 2 mL of buffer solution was added to this flask and filled to the mark with water (HPLC grade).

3) The UV-Vis spectra of actinometry samples were recorded for each time interval. The absorbance of the actinometry solution was monitored at 510 nm.

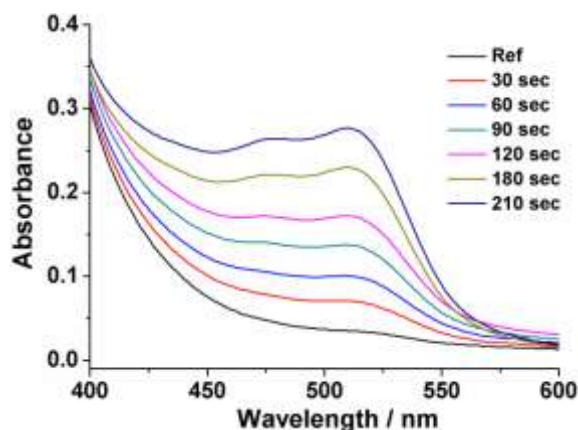


Fig. S35 The absorbance of the actinometry solution was monitored at 510 nm.

4) The moles of Fe^{2+} formed for each sample is determined using Beers' Law:

$$\text{moles Fe}^{2+} = \frac{V_1 \times V_3 \times \Delta A(510 \text{ nm})}{10^3 \times V_2 \times l \times \epsilon(510 \text{ nm})}$$

where V_1 is the irradiated volume (0.5 mL), V_2 is the aliquot of the irradiated solution taken for the determination of the ferrous ions (0.5 mL), V_3 is the final volume after complexation with phenanthroline (10 mL), l is the optical path-length of the irradiation cell (1 cm), $\Delta A(510 \text{ nm})$ is the optical difference in absorbance between the irradiated solution and that taken in the dark, $\epsilon(510 \text{ nm})$ is that of the complex $\text{Fe}(\text{phen})_3^{2+}$ ($11100 \text{ L mol}^{-1} \text{ cm}^{-1}$).

5) The moles of Fe^{2+} formed (N) are plotted as a function of time (t). The slope is a product of the photon flux (F) and the quantum yield for Fe^{2+} ($\Phi_{\text{Fe}^{2+}} = 1.13$) at 400 nm as, $F = N/\Phi_{\text{Fe}^{2+}}t$. The F was determined to be $8.97 \times 10^{-10} \text{ einstein s}^{-1}$.

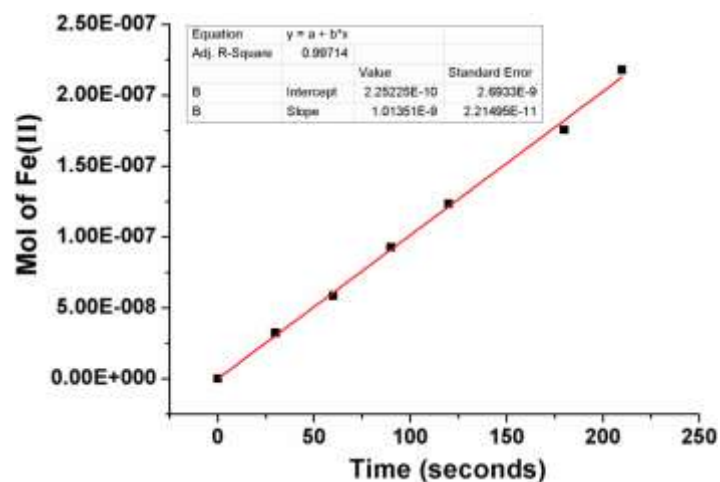


Fig. S36 The plot of the moles of Fe^{2+} as a function of time (t).

6) The moles of products formed for the reaction of interest (done by irradiating the sample alongside the actinometer solution) are described above. The moles of products formed were determined by GC measurement. The number of moles of product per unit time is related to the number of photons absorbed. The slope yields the quantum yield (Φ) of the photoreaction, 0.06.

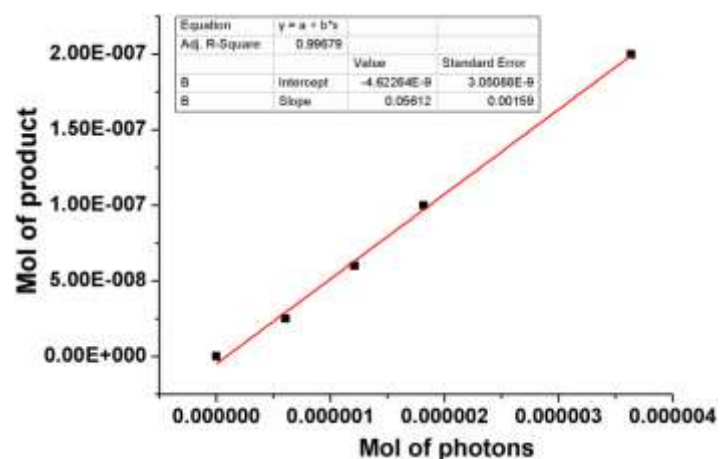


Fig. S37 The plot of the number of moles of product per unit time as a function of the number of photons absorbed.

The procedure was repeated a second time to provide a similar value, a quantum yield (Φ) of 0.08. Based on the above experiments, the observed quantum yield value ($\Phi = 0.06, 0.08$) was much lower than 1, which supports a closed photocatalytic cycle instead of a chain radical process. According to the quantum yield and reaction gas detection results, a plausible reaction mechanism was proposed for the photocatalytic cross-coupling dehydrogenation reaction of benzothiazole and diphenylphosphine oxide.

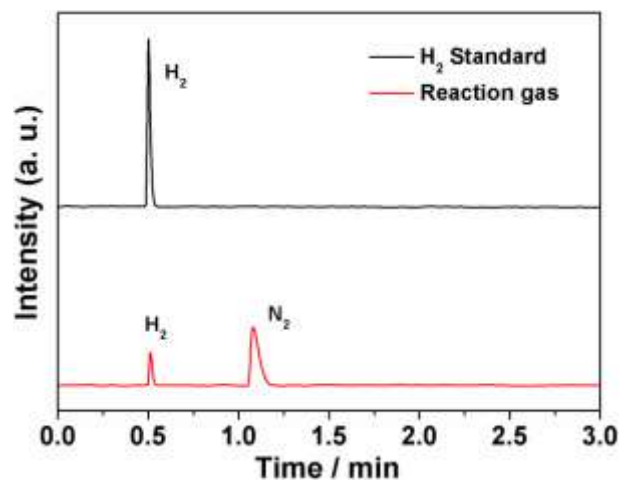


Fig. S38 The GC spectra of reaction gas.

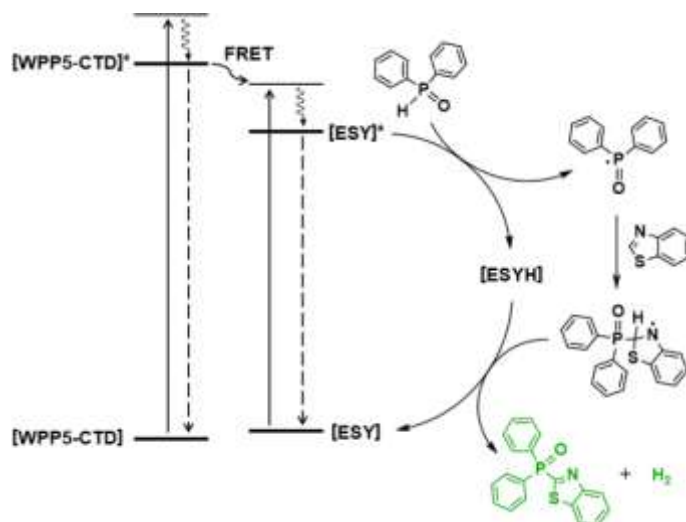
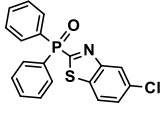
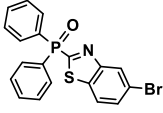
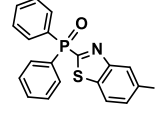
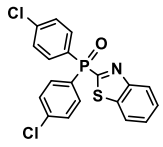
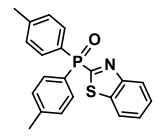
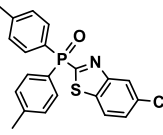


Fig. S39 The plausible mechanism for the photocatalytic cross-coupling dehydrogenation reaction of benzothiazole and diphenylphosphine oxide.

Table S3. A substrate scope for the photocatalytic cross-coupling dehydrogenation reaction of benzothiazole and diphenylphosphine oxide derivatives.

Sample	Time/h	Yield/%
	8	58%
	8	56%
	8	51%
	8	52%
	8	59%
	8	58%

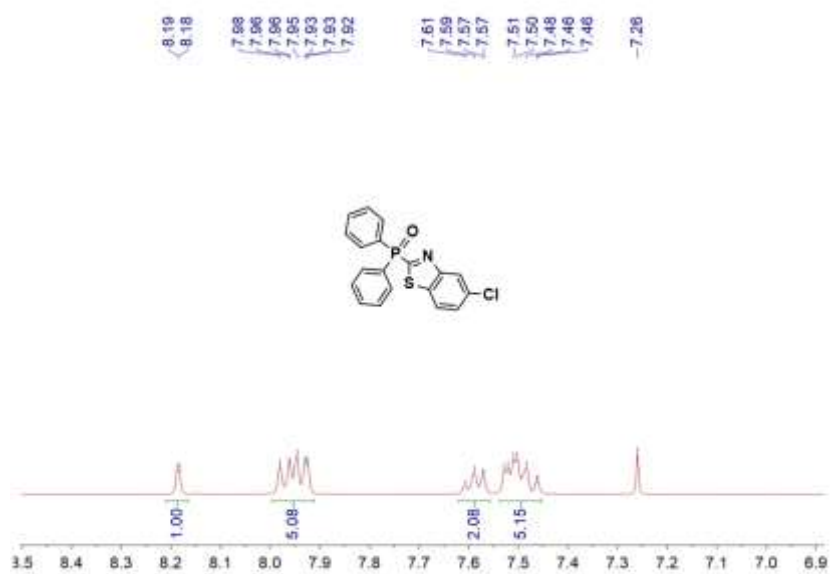


Fig. S40 ^1H NMR spectrum (400 MHz, CDCl_3 , 298 K) of the photocatalytic product.

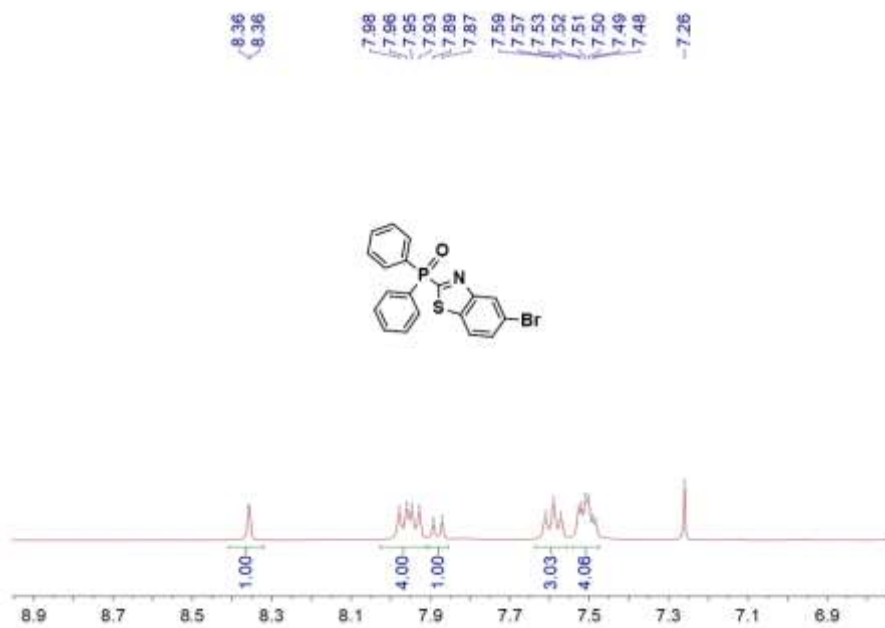


Fig. S41 ^1H NMR spectrum (400 MHz, CDCl_3 , 298 K) of the photocatalytic product.

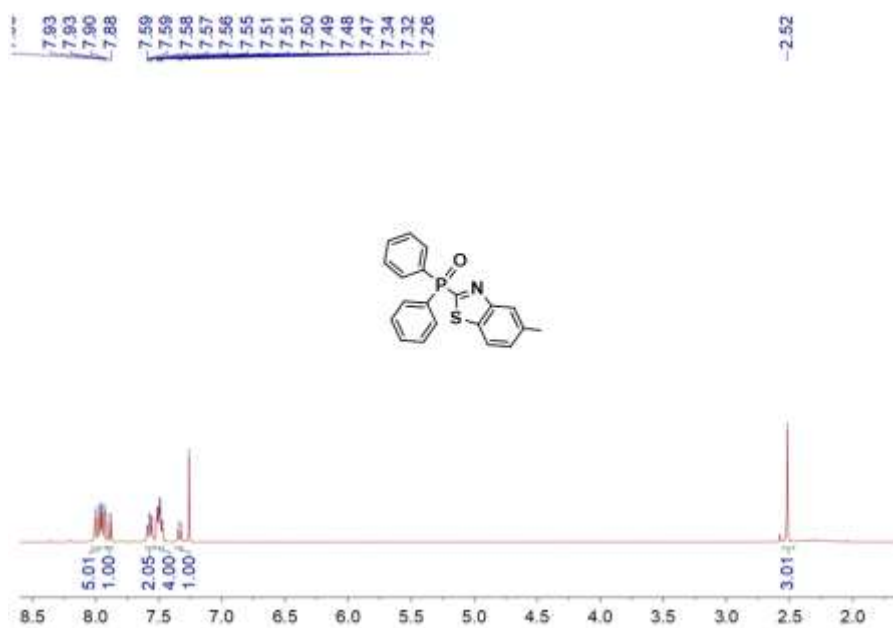


Fig. S42 ^1H NMR spectrum (400 MHz, CDCl_3 , 298 K) of the photocatalytic product.

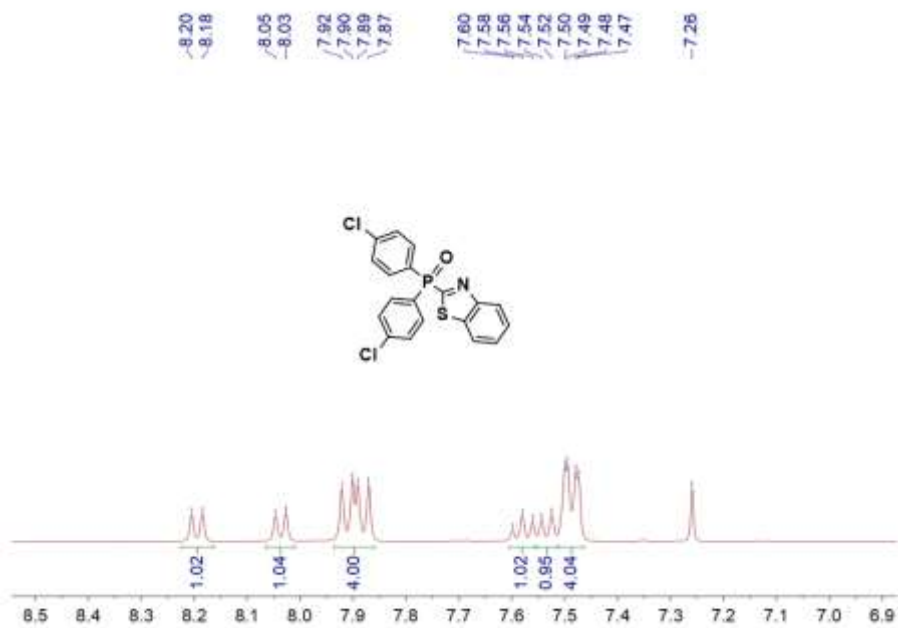


Fig. S43 ¹H NMR spectrum (400 MHz, CDCl₃, 298 K) of the photocatalytic product.

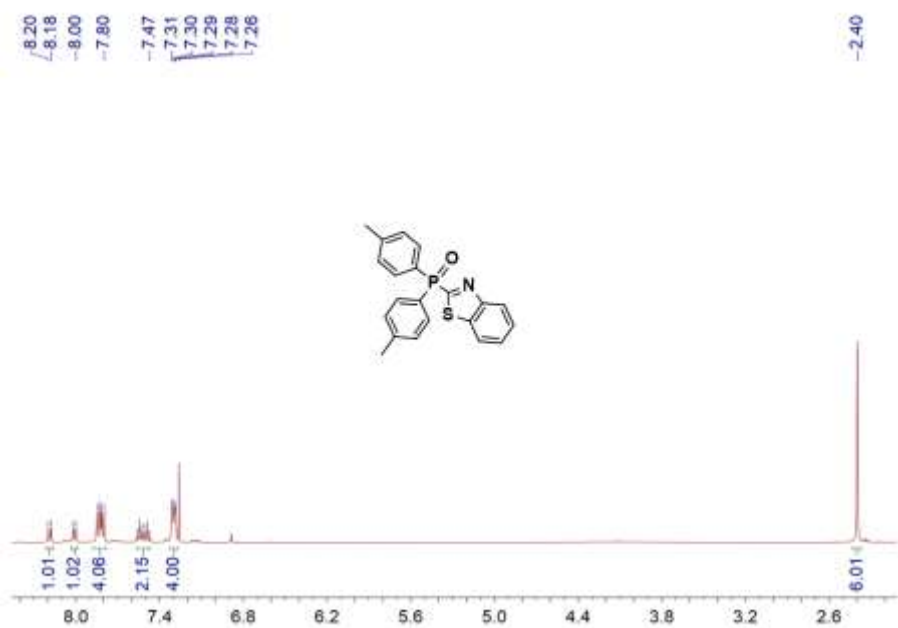


Fig. S44 ¹H NMR spectrum (400 MHz, CDCl₃, 298 K) of the photocatalytic product.

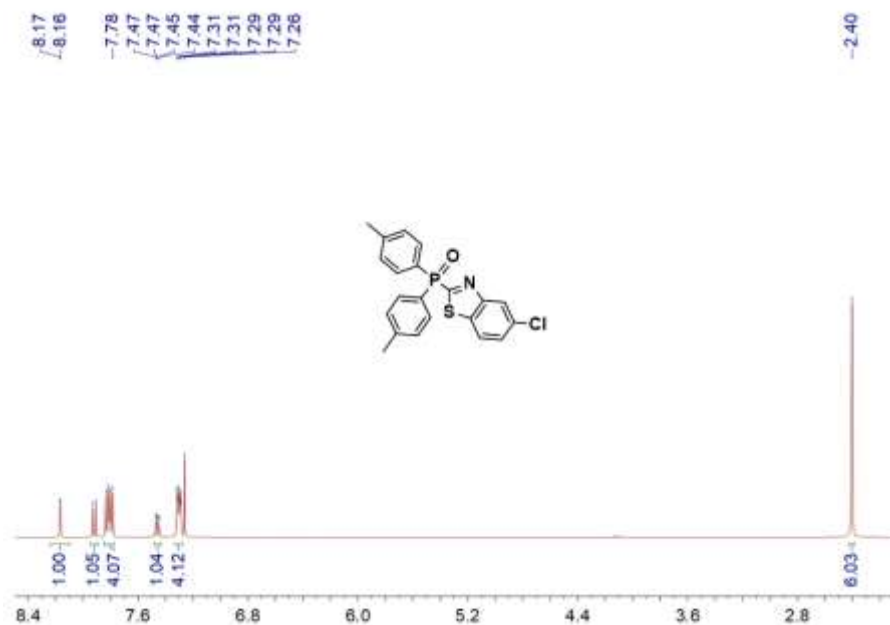


Fig. S45 ^1H NMR spectrum (400 MHz, CDCl_3 , 298 K) of the photocatalytic product.

13. References

- S1. G. Sun, W. Qian, J. Jiao, T. Han, Y. Shi, X.-Y. Hu and L. Wang, *J. Mater. Chem. A*, 2020, **8**, 9590-9596.
- S2. G. Sun, M. Li, L. Cai, D. Wang, Y. Cui, Y. Hu, T. Sun, J. Zhu and Y. Tang, *J. Colloid Interface Sci.*, 2023, **641**, 803-811.
- S3. K.-L. Wong, J.-C. G. Bünzli and P. A. Tanner, *J. Lumin.*, 2020, **224**, 117256-117265.
- S4. Y. Li, C. Xia, R. Tian, L. Zhao, J. Hou, J. Wang, Q. Luo, J. Xu, L. Wang, C. Hou, B. Yang, H. Sun and J. Liu, *ACS Nano*, 2022, **16**, 8012-8021.
- S5. Z. Zhang, Z. Zhao, Y. Hou, H. Wang, X. Li, G. He and M. Zhang, *Angew. Chem. Int. Ed.*, 2019, **58**, 8862-8866.
- S6. Y. Wang, N. Han, X.-L. Li, R.-Z. Wang and L.-B. Xing, *ACS Appl. Mater. Interfaces*, 2022, **14**, 45734-45741.
- S7. J.-J. Zhao, H.-H. Zhang, X. Shen and S. Yu, *Org. Lett.*, 2019, **21**, 913-916.
- S8. H.-H. Zhang and S. Yu, *Org. Lett.*, 2019, **21**, 3711-3715.